MODELING THE IMPACT OF THE PAYLOAD ALERT COMMUNICATIONS SYSTEM (PACS) ON THE ACCURACY OF CONJUNCTION ANALYSIS

THESIS

Landon B. Bastow, Captain, USAF

AFIT-ENV-13-M-01

DEPARTMENT OF THE AIR FORCE
AIR UNIVERSITY

AIR FORCE INSTITUTE OF TECHNOLOGY

Wright-Patterson Air Force Base, Ohio

AFIT-ENV-13-M-01

MODELING THE IMPACT OF THE PAYLOAD ALERT COMMUNICATIONS SYSTEM (PACS) ON THE ACCURACY OF CONJUNCTION ANALYSIS

THESIS

Presented to the Faculty

Department of Systems and Engineering Management

Graduate School of Engineering and Management

Air Force Institute of Technology

Air University

Air Education and Training Command

In Partial Fulfillment of the Requirements for the

Degree of Master of Science in Systems Engineering

Landon B. Bastow, BS

Captain, USAF

March 2013

AFIT-ENV-13-M-01

MODELING THE IMPACT OF THE PAYLOAD ALERT COMMUNICATIONS SYSTEM (PACS) ON THE ACCURACY OF CONJUNCTION ANALYSIS

Landon B. Bastow, BS

Captain, USAF

Approved:

/signed/	# Mar 2013
Michael R. Grimaila, PhD, CISM, CISSP (Chairman)	Date
/signed/	# Mar 2013
Jonathan T. Black, PhD (Member)	Date
/signed/	# Mar 2013
Eric D. Swenson, PhD (Member)	Date

Abstract

The Air Force Institute of Technology (AFIT) and the Air Force Research Laboratory (AFRL) are jointly developing a system known as the Payload Alert Communications System (PACS) whose purpose is to decrease the statistical uncertainty in the location of resident space objects (RSOs). PACS is designed to augment the Joint Space Operations Center's (JSpOC) existing space object tracking capabilities which is expected to increase the accuracy of conjunction estimation.

In the current PACS design, a small payload would be attached to certain RSOs prior their launch. It is envisioned that this payload would basically consist of a microcontroller, a Global Positioning System (GPS) receiver, a communication transceiver, and a power source. Once on orbit, the PACS payload would collect GPS position information and then periodically, or upon demand, transmit the orbital information back to JSpOC.

In this thesis, a study is performed to determine how the accuracy of conjunction analysis performed by the JSpOC would be impacted when RSOs are equipped with PACS. This effort requires the development an initial PACS system architecture, formulation of the mathematical models used in conjunction analysis, and the simulation and analysis of conjunction analysis under various scenarios. The results of the study reveal that PACS can significantly improve the accuracy of conjunction analysis for specific conjunctions. Additionally, an estimation of how the number of PACS equipped space objects may increase in the future is presented.

To my beautiful daughter who was
born during the writing of this thesis

Acknowledgments

There are many, many people that have contributed to this thesis, all of which I will be unable to adequately thank. However, in a feeble attempt, I would first like to thank my three advisors, Dr. Grimaila, Dr. Swenson, and Dr. Black. These three extraordinary professors were all able to constructively guide my work and give me feedback from multiple viewpoints. Not only did they share with me their extensive knowledge and expertise but they also gave me unending encouragement and support throughout the entire project.

Next, I would like to thank the individuals at the Joint Space Operational Center (JSpOC) who taught me the basics of conjunction analysis and provided me with the majority of the data that was used in this thesis. There were many people at JSpOC that gave of their time, however, Captain Stephen (Ziggy) Ziegenfuss went far and beyond in his assistance. I can say in absolute terms that without the assistance of Captain Ziegenfuss this thesis would have been a fraction of what it turned out to be.

Many thanks also go out to Mr. Seth Harvey from AFRL/SV and Dr. William Wiesel from AFIT for their support and ideas.

Last but certainly not least, I would like to thank my small family. They have been awesome partners throughout my entire time at AFIT.

Landon B. Bastow, Captain, USAF

Table of Contents

Page

Page

List of Figures

Page

Page

Page

List of Tables

Page

List of Abbreviations

AFIT……..……Air Force Institute of Technology

CA…….…. Conjunction Analysis

CM……...Covariance Matrix

CONOPS……....Concept of Operations

CSM……Conjunction Summary Message

CST……..…...Conjunction of a Serious Threat

DoD…… ……Department of Defense

DoDAF…….Department of Defense Architecture Framework

EFG……..Earth-Fixed Greenwich

GPS…….....Global Positioning System

HAC…….High Accuracy Catalog

JSpOC……..Joint Space Operational Center

OV…….Operational View

PACS……..…Payload Alert Communications System

PDF……..……Probability Density Function

POC……...….. Probability of Collision

POTUS……...President of the United States

RMS…….……....Root Mean Square

RSO……. ……Resident Space Objects

SBD…….Short Burst Data

SOS…….…….Space Object Self-Tracker

SP……...……Special Perturbation

SSN……...Space Surveillance Network

STK……... Systems Tool Kit

TCA…….……Time of Closest Approach

USG……...……..United States Government

MODELING THE IMPACT OF THE PAYLOAD ALERT COMMUNICATIONS SYSTEM (PACS) ON THE ACCURACY OF CONJUNCTION ANALYSIS

I. Introduction

1.1 Background

One of the most significant problems that the Department of Defense (DoD) encounters in space operations is the potential for collisions, also called conjunctions. The first man-made object was placed into orbit approximately 55 years ago with the Russian launch of Sputnik. Since that time, the number of Resident Space Objects (RSOs) has grown exponentially. Initially, there was little concern of two RSOs colliding due to the relatively few orbiting objects and the vastness of space. However, due to the dramatic and continuing increase in RSOs over time, the risk of collision has grown. A recent example of a collision is the February 2009 collision between the active Iridium 33 satellite and the defunct Cosmos 2251 satellite. The consequences of this collision were not only the destruction of a multimillion dollar Iridium satellite, but also the creation of thousands of new pieces of space debris, each which must be closely monitored in order to avoid additional collisions with active satellites [1]. Figure 1 shows how the number of RSOs increased during the time period from 1956 until 2010. Note that the dramatic spike of fragmentation debris in 2009 is the result of the Iridium/Cosmos collision.

The number of RSOs in space has become a serious concern for military space operations. In 2010, the Honorable William J. Lynn, Deputy Secretary of Defense for the United States, said in a speech at the U.S. Strategic Command Space Symposium that

space has become “congested, contested, and competitive.” Lynn continued by saying that, “the skies over earth are so cluttered with debris that further collisions could eventually put some usable orbits in jeopardy.” He further stated that our ability to use space to our advantage is paramount for the continued security of the United States and that, “we are approaching a point at which the limitless frontier no longer seems quite so limitless” [2].

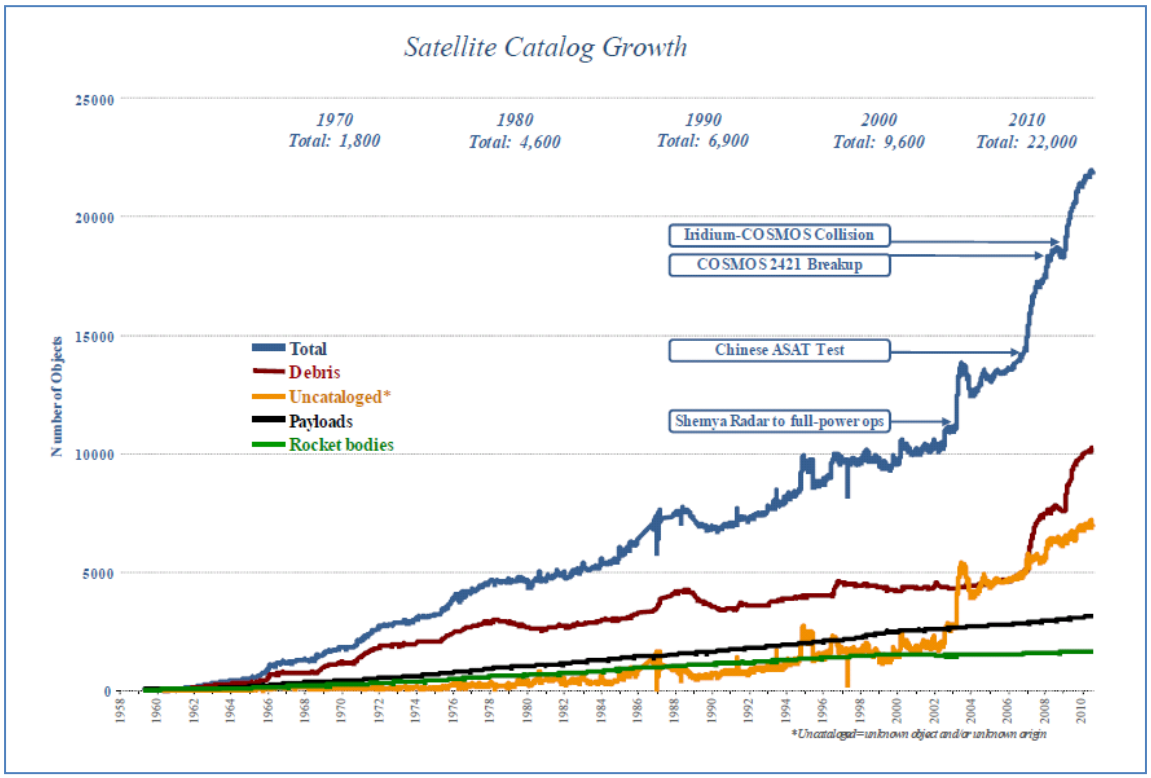

Figure 1: Satellite Catalog Growth - Number of Objects in Earth Orbit by Object Type [3]

For the United States Government (USG), the organization in charge of monitoring space for potential collisions is the Joint Space Operational Center (JSpOC), headquartered at Vandenberg Air Force Base in California. The JSpOC has an extensive network of ground based assets known as the Space Surveillance Network (SSN) that

observe space in order to detect, track, and identify man-made objects in space. The JSpOC uses the observations collected from the SSN to estimate the orbital information of the thousands of RSOs and uses the information to mathematically predict where those RSOs will be in the near future. Using this information, JSpOC is able to identify and monitor potential future collisions, a process known as conjunction analysis (CA).

If a potential conjunction is predicted as defined by the JSpOC, it notifies the involved satellite operator(s) so they can make a decision whether or not to maneuver to avoid the chance of a potential conjunction (assuming that at least one of the involved RSOs has the ability to maneuver) [1]. This maneuver decision of the satellite operator is largely based upon the perceived risk of collision which is primarily a function of the uncertainty in the estimated location of the two objects at the time of conjunction. The operator must weigh this risk against the resources required to maneuver.

Predicting whether a collision will actually occur is extremely difficult and computationally expensive. One of the primary difficulties in CA is that there is always a certain degree of uncertainty surrounding the actual position and velocity of the colliding objects at the time that they are most likely to collide, known as the time of closest approach (TCA). For example, at the TCA, the JSpOC may estimate that two objects will pass by each other with a separation of approximately 50 m. However, due to the uncertainty of where the satellites will actually be at the TCA, this actual distance may be as small as 0 m (a collision) or as much as thousands of meters (a far miss).

Satellite operators are typically limited in how often they are able to maneuver their satellites due to a limited fuel supply. Therefore, satellite operators perform a cost-

benefit analysis to determine if they should perform a maneuver. As an example, if a satellite operator believes there is a one-in-a-million chance (i.e., a 0.0001% chance) of a collision between the satellite and an RSO, the operator may decide not to maneuver because the odds of collision are extremely low and therefore is not worth the fuel expenditure. However, if the operator believes there is a one-in-ten chance (i.e., a 10% chance) of collision, then the operator would be much more likely to decide to maneuver (assuming that the satellite has the capability to maneuver). In order to not waste fuel, satellite operators attempt to minimize the number of unnecessary maneuvers. Operators strive to minimize the number of false-positive maneuver decisions (a collision is predicted and therefore a maneuver is made, however a collision would not have occurred even if an avoidance maneuver wasn't made) and false-negative maneuver decisions (an avoidance maneuver is not made and a collision does occur).

As an example, suppose a satellite operator believes that there is a one-in-a-thousand chance (i.e., a 0.1% chance) of collision between their satellite and a piece of debris. The satellite operator has a decision to make: to maneuver out of the way of the debris or not. If the operator chooses to maneuver but a collision would not have occurred regardless, then the operator made a false-positive maneuver decision (resulting in the satellite's fuel being wasted). However, suppose the operator chooses not to maneuver and instead risks the collision (believing that 999 times out of 1000 a collision will not occur). If a collision occurs due to the inaction, then a false-negative maneuver decision would have occurred. Basically, a false-positive maneuver decision results in a needless waste of valuable fuel, where a false-negative results in the partial or total

destruction of the satellite and potentially hundreds of additional pieces of space debris. Obviously, minimizing both the false positives and false negatives is very important to the individual space operators and entire space community.

To address this concern, the Air Force Institute of Technology (AFIT) and the Air Force Research Laboratory (AFRL) Space Vehicles Directorate are jointly developing a system known as the Payload Alert Communications System (PACS) which is designed to decrease the uncertainty involved with the satellite positions for certain space objects. One of the primary goals of this system is to improve the accuracy of JSpOC's conjunction analysis by reducing the uncertainty in RSO position information thereby decreasing the prevalence of false-positive maneuver and false-negative maneuver decisions.

It is important to note that the PACS system is very early in its development and is pre-operational. AFIT and AFRL are in the process of building the first prototype to demonstrate the proof of concept. This experimental prototype is referred to as Space Object Self-Tracker (SOS) which falls under the PACS program. In other words, PACS is the overarching program ran by the AFRL/SV directorate, and SOS is the prototype being built primarily by AFIT to demonstrate proof of concept for the PACS program. This thesis will focus on the potential impacts of the PACS system and not the development of the SOS prototype. The details of the SOS experiment are outside the scope of this thesis and therefore the details of this prototype will not be explored in this text.

In the current preliminary design of the PACS system, a relatively small payload (hereafter referred to as a PACS payload) would be attached to certain RSOs prior their launch. It is envisioned that this payload would basically consist of a microcontroller, a Global Positioning System (GPS) receiver, a communication transceiver, and a power source. Once on orbit, the PACS payload would collect GPS position information and then periodically, or upon demand, transmit the position information back to JSpOC through its communication transceiver over a commercial satellite constellation. For the purposes of this thesis it is assumed that the Iridium satellite constellation would be used to facilitate the communications between the PACS payload and the JSpOC. Figure 2 shows the physical structure of an early design concept of the PACS payload.

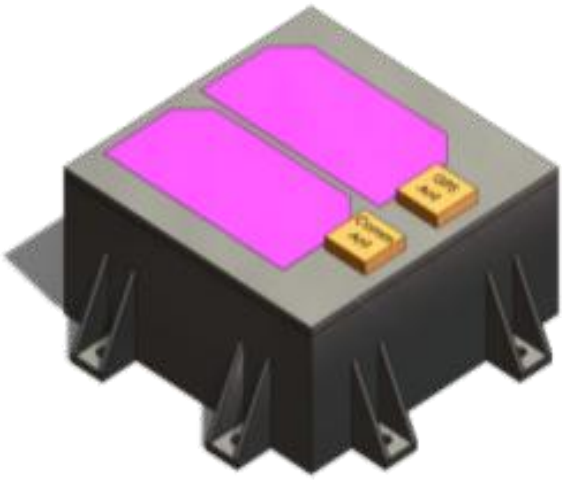

Figure 2: Depiction of a Possible PACS Payload Design. Approximate size: 10 cm x 10 cm x 5 cm. Source: Air Force Institute of Technology – Department of Aeronautics and Astronautics.

It is anticipated that the satellite position uncertainty of a RSO with a PACS payload can be reduced significantly when compared to the current ground-based tracking abilities of the SSN. This system will enable the JSpOC to provide more precise

data to the involved satellite operators. These operators would then be in a much better situation to decide whether or not to maneuver the satellite to avoid a collision, thereby reducing the number of false-positive and false-negative maneuvers. If the PACS system is incorporated into the JSpOC conjunction analysis architecture, it would mean a paradigm shift of how objects are tracked and monitored. Basically, currently RSOs are typically tracked remotely from the ground based SSN. Where, if PACS is fielded, then those RSOs with a PACS payload would report their own position to the JSpOC on a periodic or on-demand basis.

1.2 Problem Statement

The growing number of RSOs, combined with limitations in accurately tracking the position of each RSO, yield conjunction analysis results that are not accurate enough to adequately inform satellite operators of the risk of collision leading to too many false-positive and false-negative maneuver decisions. In this thesis, a study of the existing JSpOC conjunction analysis methodology is presented followed by an analysis of how the accuracy of conjunction analysis might be improved by incorporating the PACS system.

1.3 Research Goals

This thesis is focused on first understanding how conjunction analysis is conducted, modeling the existing conjunction analysis process, and quantifying the improvement in conjunction analysis when incorporating the PACS system to the existing JSpOC architecture. Specifically, the research goals addressed in this thesis are listed below:

1. Establish a baseline system architecture for a PACS system using the Department of Defense Architecture Framework (DoDAF).
2. Define conjunction analysis and explain the way it is currently conducted at JSpOC.
3. Estimate the existing tracking capabilities of the JSpOC to track RSOs.
4. Estimate the potential accuracy of a PACS payload.
5. Model the differences in the Probability of Collisions (POCs) between a conjunction where PACS system is incorporated ("could-be") and where PACS is not incorporated ("as-is").
6. Estimate the number of RSOs that could potentially incorporate a PACS payload over a ten year period after the system was operational.
7. Estimate the how often RSOs that could potentially have include a PACS payload experience a near conjunction.

1.4 Assumptions/Scope/Limitations

There are several technical and system challenges that must be addressed and overcome before the fielding of the PACS system. However, the primary purpose of this thesis is to analyze the potential benefits of the PACS system assuming that the system could become operational. Therefore, this thesis will focus primarily on evaluating the benefits that the PACS system could provide to JSpOC (and ultimately the entire space community) assuming that all technical and programmatic hurdles could be eventually overcome. An example of technical challenge that will not be addressed in this thesis is the way in which the PACS system will be powered. The challenge to provide sufficient electrical power will be dependent upon multiple variables including the type of RSO (i.e. is the RSO an active satellite that creates its own power independent of the PACS payload or is it a rocket body that has no power creation capabilities) and the operational

mode of the PACS payload (i.e. does the PACS payload collect GPS data and transmit over the Iridium network once, twice, dozens, or hundreds of times of day or only on-demand) which has not yet been determined. Making the "it could technically become operational" assumption will allow this thesis to focus primarily on analyzing the performance benefits of the system.

Additionally, there are multiple possible applications for the PACS project that extend beyond conjunction analysis. However, for the purpose of this thesis, the only application that will be studied is the ability to improve the accuracy of conjunction analysis.

One of the primary limitations in studying a system that is still being developed is that the precise capabilities of the system are largely yet to be determined. Therefore, the PACS system performance will be modeled with several key performance assumptions which will be identified in future chapters.

One of the primary research goals of this thesis is to quantify the existing tracking capabilities of the JSpOC. Understandably, a military organization such as the JSpOC is cautious in disclosing large amounts of data regarding their capabilities for operational security reasons. Therefore, the quantity of data obtained for the JSpOC is intentionally small (data on 15 conjunctions). These limitations of this small data set are further discussed in Chapter III.

The PACS system, as currently envisioned, would communicate with the JSpOC over the Iridium commercial communication satellite network. It is likely that besides Iridium network there may be other communication systems that could be used.

However, for purposes of this thesis it is assumed that the Iridium communication network will be the only communication network used by PACS. It is also assumed that a PACS enabled RSO would need to have an orbital perigee below 750 km in order to communicate with the Iridium network. This assumption is made because the Iridium satellites are at approximately 781 km altitude and their communication beams are pointed towards Earth. Therefore, it is assumed that RSOs would need to be at an altitude below the 781 km in order for communication to occur. The 750 km level is an estimation that will need to be studied in the future once the interface between the PACS payload and the Iridium network is better understood. This interface is currently being studied at AFIT. An additional assumption made for this thesis is that the PACS payload will be attached to future RSOs that have not yet launched. This assumption is based upon the supposition that the cost to put a PACS payload on an already orbiting RSO is prohibitive. Accordingly, for this thesis, it is assumed that the only objects that could incorporate a PACS payload are RSOs that have not yet launched and will have an orbital perigee below 750 km.

1.5 Methodology

The primary methodology used in this thesis to answer the research questions is analytical modeling and simulation. Two primary sources of data were used in this thesis. The first data source was a limited set of historic conjunction data acquired from the JSpOC. The second data source was obtained from the unclassified website www.beta.space-track.org. The process of obtaining this data and its format is explained in detail in Chapter III.

Multiple computer tools used to conduct the research presented in this thesis: a mathematics program called MATHCAD; Microsoft Office including Word, Excel, and PowerPoint; the systems architecture program called Enterprise Architect; and the satellite modeling program Systems Tool Kit (STK). After obtaining the necessary software programs and data, one of the first steps was to create a process to calculate the Probability of Collision (POC) based upon a given conjunction. New code was written by the researchers in MATHCAD that was able to calculate the POC of the historic conjunctions provided by JSpOC. This code is provided in the Appendix. These calculated POCs were then compared with the POCs calculated by JSpOC. Next, the conjunctions were manipulated to model the potential difference of incorporating a PACS payload (As-Is versus Could-Be). This process and its results are described in great detail in Chapters III and IV.

The number of potential PACS enabled RSOs was estimated largely with data provided from the www.beta.space-track.org website. This website provides a current database of the unclassified objects tracked by JSpOC. Included in this database are historic information of the number of launches by orbit type, launching country, and object type. By studying previous launches of RSOs, the researchers were able to estimate future launches and thereby estimate the number of PACS enabled RSOs over a certain time period after the system becomes operational.

1.6 Research Impact

This thesis aims to study the impacts that the PACS system could potentially have on the JSpOC's accuracy of conjunction analysis. Ideally, the analysis presented in this

thesis and its corresponding results will provide useful information to the decision makers of the PACS system in support of the management of the program.

1.7 Document Preview

This thesis consists of five chapters. This first chapter gave an overview of this thesis project. Chapter II explains the necessary background information. Chapter III describes in detail the research methodology used. Chapter IV contains the results of the research described in Chapter III. Finally, Chapter V presents the conclusion based upon the results and provides recommendations for future research.

II. Background

2 Chapter Overview

This chapter will describe the necessary background that supports the methodology, research and conclusions in the future chapters. The topics covered include a discussion on the basics of the Payload Alert Communications System (PACS) project including a brief description of the systems that will be used to support PACS. Also included in this chapter is the background on performing conjunction analysis (CA).

2.1 PACS Systems Engineering and Systems Architecting

In this section, the purpose of Systems Engineering and Systems Architecting as it relates to the PACS system will be described.

First of all, systems engineering is an interdisciplinary, top down approach to realizing a successful system. It is focused upon integrating all disciplines and specialties into a concerted and structured development process that addresses the entire lifecycle of a problem [6]. Systems architecting is a sub-skill of systems engineering. The architect is responsible for organizing the system components, guiding principles and relationships between components and the external environment. The fundamental outcome of systems architecture is a successful mission or vision. The architecture itself is a means to an end and should be tailored to fit the purpose. Formal systems architecture is designed to promote interoperability and support decision-making processes and solutions.

Systems Engineering and Systems Architecture processes together are particularly useful for emerging technology due to their interdisciplinary nature and use of best practices over the entire lifecycle of a project. Applying architectural rigor to defining a

system visualizes the practical implementation aspects and allows the user and architect to work together to decide upon the level of abstraction most useful in a tailored analysis.

In order to adequately design a complex system, such as PACS, a rigorous Systems Engineering process is required. Systems can be described as "a collection of different things that together produce results unachievable by the elements alone" [6]. A systems engineer understands that the various components within a system must be taken into account when developing architecture for a new or existing system. When architecting a system, the system architect must approach by focusing on the system as a whole when searching for a solution.

The principle guide for the Department of Defense (DoD) in creating architectures for a system is called the DoD Architecture Framework (DoDAF). There are multiple viewpoints from which the system can be architecturally described. These different viewpoints interrelate to create a whole-system concept for the complex system. Figure 3 shows the DoDAF viewpoints emphasizing the interrelationships between the views [12]. As part of the research of this thesis, several high level system architecture views of the PACS system were created. These views will be described in future chapters with the exception of the Operational View – 1 (OV-1) which will is shown in this chapter to aid in the overview description of the PACS system and necessary sub-systems.

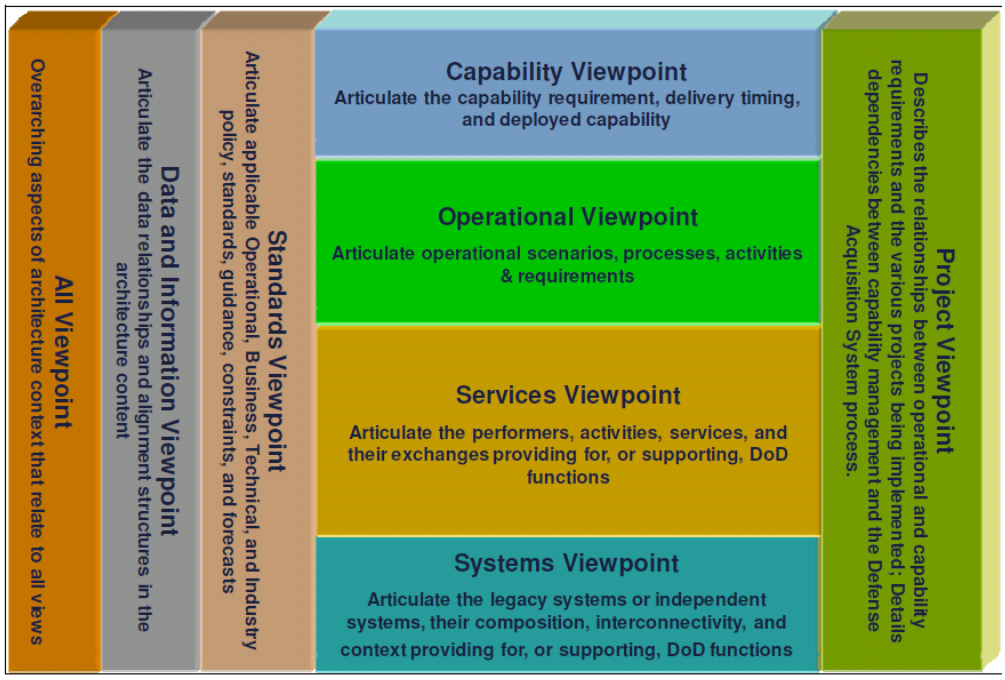

Figure 3: DoDAF Viewpoints Emphasizing the Interrelationships Between Views [12]

In order to properly map out the PACS system, an initial system architecture needs to be established. By using the previously discussed DoDAF, certain views were chosen to be developed as part of this thesis. As the system evolves, the DoDAF views will obviously evolve and additional views will be created. Since the PACS system is in the very initial stages of development, the focus was on a high level Concept of Operations (CONOPS) and the Operational Viewpoints (OV) which best define the high level operational use of the system. For the purposes of this research, the following DODAF views were created: OV-1, OV-2, OV-5a, and OV-6. These views were selected because they provide a high level view of the operation of the PACS architecture. It is important to note that this is not the complete system architecture, but instead a collection of views that will clarify the system as a whole.

The OV-1 is the high-level graphic of the speculated operational concept. This graphical architectural view presents the systems main concepts and unique aspects of operations. It primarily depicts interactions between the architecture and its environment as well as between the architecture and external systems.

The OV-2 is the operational resource flow diagram. This high level diagram show how the resources (in this case the flow of data) of the PACS system flow through the entire system.

The OV-5a is the "Operational Activity Decomposition Tree" which shows the operational activities organized in a hierarchal structure. It describes operational activities that are required for the system to achieve it primary operational objectives.

The final architecture view created was the OV-6c which is known as an "Operational Event-Trace Description." The OV-6c provides a time-ordered examination of the resource flows for one or more scenarios of interest. Operational Event/Trace Descriptions, sometimes called sequence diagrams, event scenarios, or timing diagrams, allow the tracing of actions in a scenario or critical sequence of events.

2.2 PACS's Notional Concept of Operation

In this section, a very high level concept of how the PACS system could possibly be used operationally is presented. Several of the support systems described in this section will also be described in further detail as necessary later in this thesis. As an overview of the operational purpose of the PACS system, the purpose of the system is to self-report orbital information directly to JSpOC by leveraging the capabilities of the Iridium satellite network and the GPS network. This orbital information could then be

used in combination with the orbital information already obtained from the SSN. The union of the information from the PACS system and the SSN could then produce a more accurate orbital estimation for the JSpOC to perform superior analysis of possible conjunctions.

It is envisioned that the PACS payload would receive GPS data from its on-board GPS receiver. The PACS payload would then take this GPS information from multiple GPS signals in order to determine its position, similar to how a GPS unit in an automobile determines its position on the surface of Earth. The obvious differences between a GPS receiver on an automobile and a GPS receiver on a PACS payload is that the PACS payload is at a much higher altitude (approximately between 300 km and 750 km) and traveling at much higher speeds (around 7 km/s). Fortunately, GPS receivers have been used operationally for years in space for orbital determination purposes [4]. The next step would be to transmit the orbital information of the RSO (derived from the received GPS data) to JSpOC through the Iridium network.

The JSpOC would use this PACS supplied orbital information in addition to the data obtained from its existing SSN to increase the precision of the orbital estimate of the RSO. With a more accurate estimate of the RSO, JSpOC's ability to predict a conjunction would be increased. Figure 4 shows an illustration of the high level concept of operations (CONOPS) of the PACS system. This view is referred to as the Operational View - 1 (OV-1).

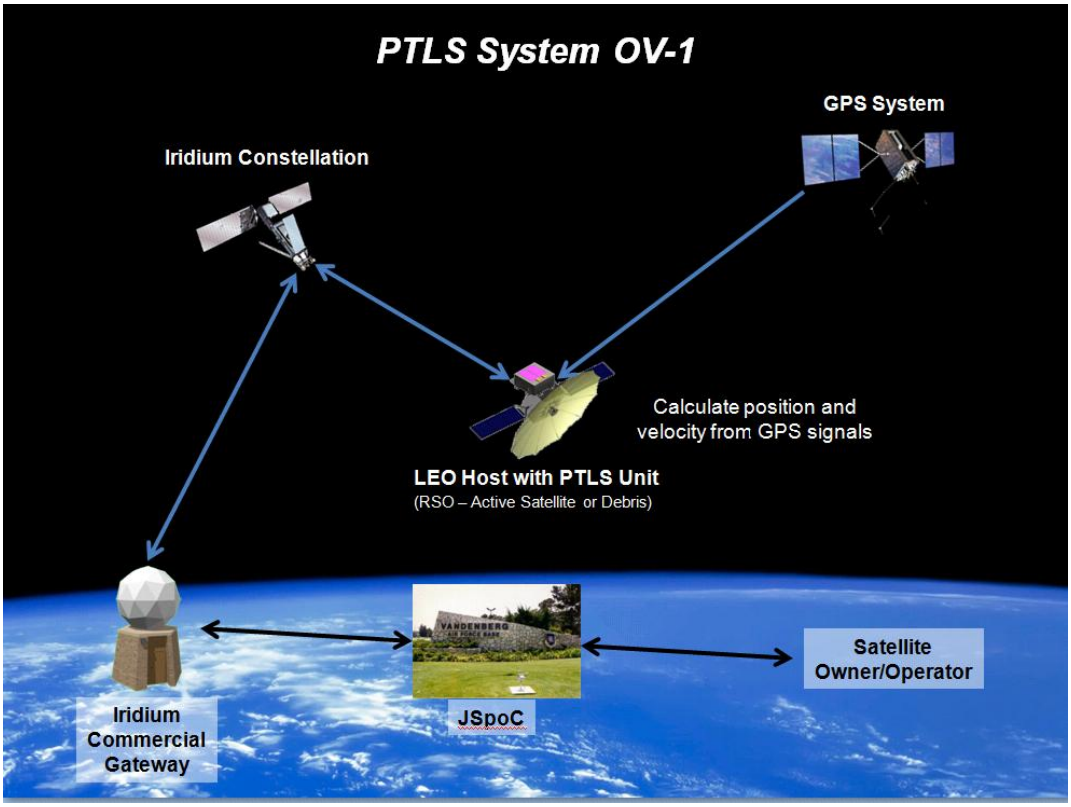

Figure 4: PACS Operational View – 1 (OV-1)

2.3 Uncertainty in Orbital Position

This section describes the difficulties involved in predicting orbital locations for RSOs. The uncertainty in predicting where a RSO will be in the future is due to two sources: measurement errors and propagation errors.

The measurement error is due to the limitations of the sensors to precisely identify the object's exact location at the time of the observation. In part, this accuracy is limited because orbiting objects in LEO are traveling at very high speeds and are typically hundreds of kilometers away from the sensor.

The second source of error is due to the difficulty of propagating orbital positions forward in time. Exact propagation is nearly impossible because even extremely small

errors in estimating the perturbations of the orbit of an RSO accumulate overtime. For example, the largest source of uncertainty for objects in LEO is due to the variance in atmospheric drag. The atmospheric drag is difficult to estimate and predict because the atmospheric density is variable. Therefore, when JSpOC is predicting the position of a satellite days in the future, it has to predict the effect of multiple variables, which consequently create uncertainty in their estimate on the future RSO position [1].

2.4 Joint Space Operations Center (JSpOC)

The primary user of the PACS payload data would be the JSpOC. The JSpOC is headquartered at Vandenberg AFB in California. Figure 5 shows the command relationship from the President of the United States (POTUS), to the Commander of USSTRATCOM, to the Commander JFCC-Space who has command over the JspOC [1].

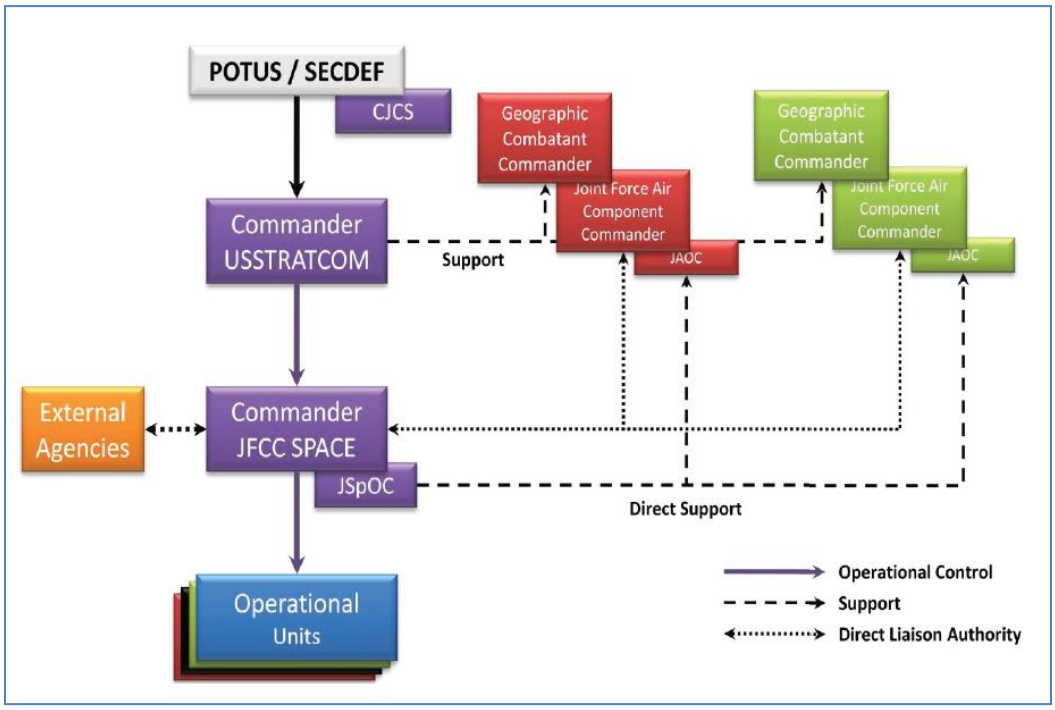

Figure 5: Command Relationship from POTUS to JSpOC [1]

The man-made RSOs for which JSpOC monitors can be divided into two broad categories, namely, active satellites and space debris. An active satellite is any object in space that is currently operational. Space debris (or just "debris") is defined as any object that serves no operational purpose. Examples of debris include dead satellites, rocket bodies, bolts, and even paint chips. JSpOC can track objects that are as small as a baseball – approximately ten centimeters diameter. Of these 22,000 RSOs, only about 5% are active satellites (approximately 1000 active satellites); the other 95% consist of rocket bodies (8%) or fragments and inactive satellites (87%) [3]. Depending on its orbit, space debris may reside in space for years, decades, or even millennia before reentering Earth's atmosphere and disintegrating. Unless disposed of through different means, these objects continue to pose a threat to operational satellites.

2.5 Space Surveillance Network

This section describes the current methods used in space operations for determining the orbital information of a RSO. For the United States, the main source of tracking all RSOs (active satellites and debris) is through the Space Surveillance Network (SSN), which is managed by the JSpOC.

The JSpOC tasks their worldwide network of sensors to track orbiting objects. Some of the SSN's 29 sensors are used exclusively to track RSOs (dedicated sensors), while others have a different primary mission (contributing and collateral sensors) and provide RSO orbit information whenever that mission is not superseded by their primary mission. The SSN, with their 29 worldwide sensors take between 380,000 and 420,000 observations each day [6]. Since the launch of Sputnik in 1957, there have been over

38,000 man-made objects that have been tracked and catalogued. Of those 38,000, approximately 22,000 are still in orbit and tracked by the SSN [6]. Figure 6 shows the SSN resources around the world, marking the sensors that are dedicated, contributing, and collateral.

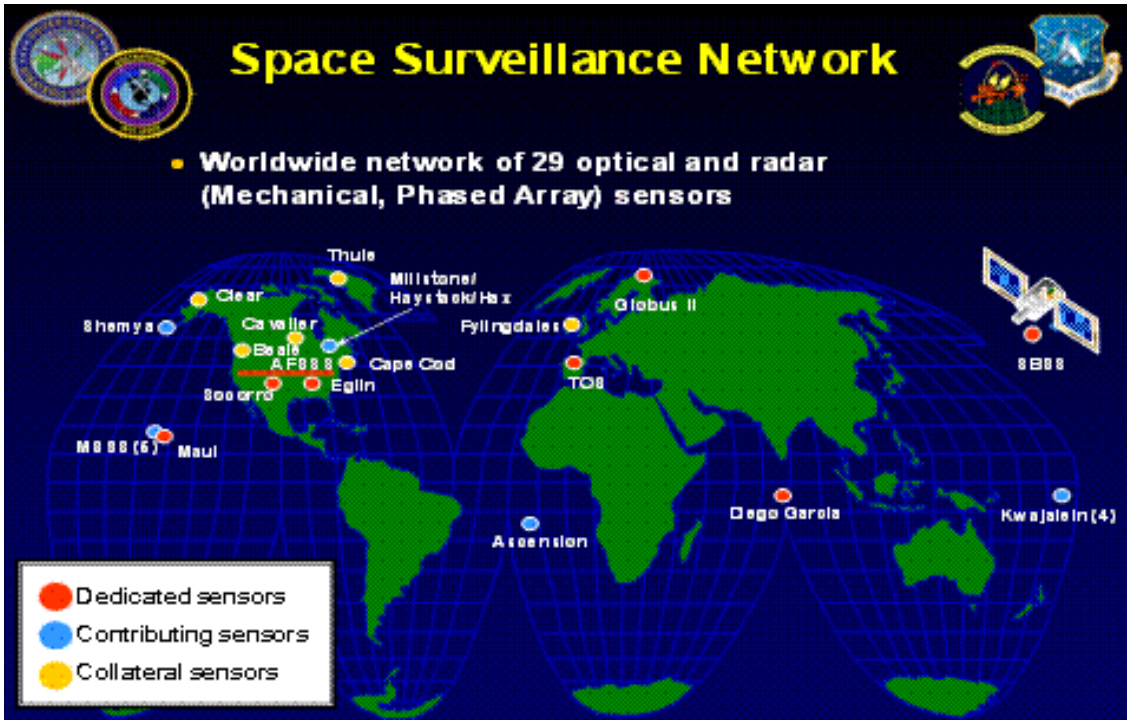

Figure 6: JSpOC's Space Surveillance Network [3]

2.6 Conjunction Analysis

The resources to fully monitor and analyze these objects are limited. Colonel Wasson, Chief of the Combat Operations Division at JSpOC, discussed the difficulties of performing Space Situational Awareness (SSA) at the 2010 SSA conference, saying that "current SSA capabilities are insufficient to maintain pace with an increasingly difficult and challenging environment." [4]

If the resources to monitor potential space conjunctions were limitless, all objects, both active and inactive, could be constantly monitored and all potential conjunctions would be tracked. Unfortunately, resources are limited and therefore JSpOC makes the most efficient use of its assets to best inform the satellite operators of potential collisions. JSpOC currently does not monitor potential collisions between two inactive space objects; this type of conjunction monitoring is referred to as an "All-on-All" analysis. Instead, JSpOC performs what is called an "All-on-Active" analysis, meaning that JSpOC monitors only active satellites (to include all government, foreign, and commercial satellites) against the entire catalog of space objects for conjunctions [5].

To perform this "All-on-Active" analysis, JSpOC currently uses the orbital information obtained from the SSN. Once the SSN information is digested at JSpOC, all tracked objects are cataloged in what is called the High Accuracy Catalog (HAC). JSpOC uses the information in the HAC to propagate the objects forward in time to screen for any potential conjunctions. This screening process typically looks forward in time approximately 5-10 days and propagates all active satellites against all objects (both active satellites and debris). If a potential collision is identified, JSpOC may notify the specific owner/operator and may task the SSN to make extra observations of both objects to obtain more accurate information regarding orbital position. A complete CA is typically performed once a day [5].

To propagate objects forward in time to predict collisions, JSpOC uses a high-accuracy orbital propagation model, known as Special Perturbation (SP) [4]. The SP model numerically integrates the equations of motion to include all high order perturbing

accelerations. The SP model not only estimates the position of the object propagated forward in time, but it also provides information on the uncertainty of the estimate in the form of the covariance matrix (CM).

2.7 Conjunction Summary Messages

If a potential conjunction is identified, between an active satellite and any other RSO (active satellite or debris), JSpOC informs the operator of the involved satellite if certain thresholds are met. JSpOC provides information on the upcoming potential conjunction through what is called a Conjunction Summary Message (CSM). For satellites in LEO, a CSM is created and transmitted to an owner/operator if all of the criteria listed in Table 1 below are met [1].

Table 1: JSpOC Criteria for Transmitting a CSM

1. Conjunction occurring in the next 72 hours
2. Overall miss distance is less than 1000 meters
3. Miss distance in the radial direction is less than 200 meters
4. At least one of the two involved RSOs is an active satellite

If all of the criteria in Table 1 are met, a CSM is sent to the involved satellite operator(s) to make him or her aware of the potential conjunction. Among many other pieces of data, the CSM provides the position and velocity vector and the 3 x 3 covariance matrix for both of the colliding RSOs. All of the information in the CSM is propagated forward in time to the Time of Closest Approach (TCA).

When JSpOC identifies a conjunction, a Probability of Collision (POC) calculation is made by JSpOC. This POC however is not provided as part of the CSM. Each operator is responsible to assess the risk of collision and decide whether they will maneuver to attempt to mitigate the risk [1].

2.8 Coordinate Systems Used in the CSMs

There are two primary coordinate reference frames presented in the CSMs: Earth-Fixed Greenwich (EFG) reference frame and the asset centered UVW reference frame. In the CSM, the covariance matrix is provided in the object's specific UVW frame, while the position and velocity vectors are in the EFG frame. Both coordinate systems will be briefly described in this section.

The UVW coordinate system is asset centered, meaning the coordinate system is centered upon the asset. The components are displayed in order of the Radial (U), In-Track (V), and Cross-track (W). The U ("Radial") is the unit vector in the geocentric radial direction. The W ("Cross-track") is the unit vector that is in the direction of the satellite's angular momentum which perpendicular to the satellite's orbit plane. The V ("In-Track") is the unit vector that is equal to the cross product of U and V components. Figure 7 shows a description of the UVW reference frame.

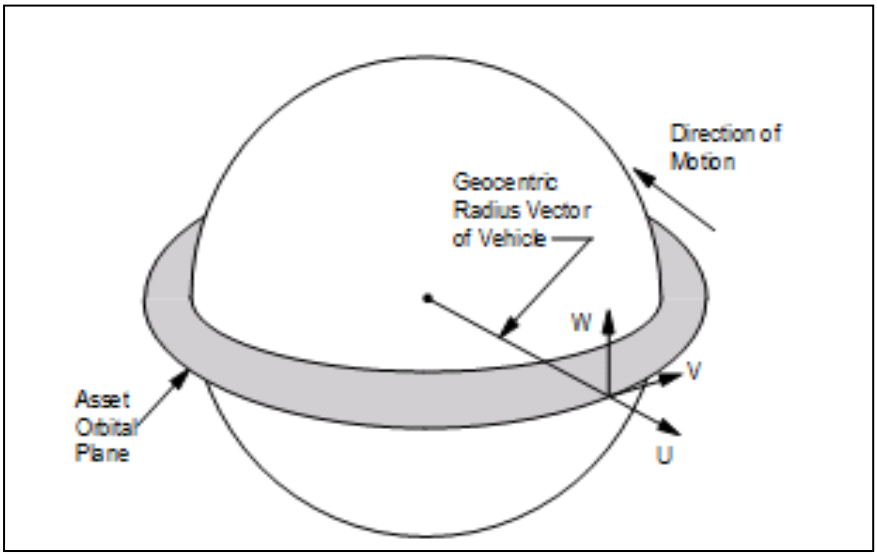

Figure 7: UVW Reference Frame

In contrast, the position and velocity of the RSOs are given the EFG coordinate system. Unlike the UVW reference frame, the EFG frame is centered on the center of mass of the Earth. The EFG frame is represented in X, Y, and Z components. The X component intersects the surface of Earth at 0 degrees latitude (Equator) and 0° longitude (Greenwich). The Y component intersects the surface of the Earth at the equator and 90° East longitude. Finally the Z component points towards north normal to the equatorial plane. The difference between the EFG reference frame and an Earth centered inertial systems is the EFG system rotates about the Z axis as the Earth rotates. Figure 8 shows a diagram of the EFG coordinate system.

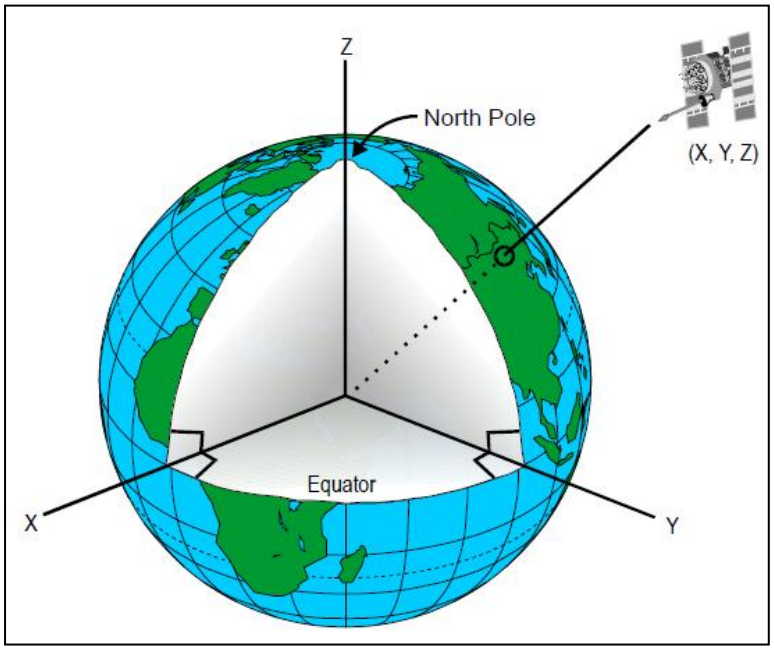

Figure 8: Earth Fixed Greenwich (EFG) Reference Frame

2.9 Iridium Network

As mentioned earlier, for the purpose of this thesis that the Iridium satellite network will be the primary means of communication between the PACS payload and the JSpOC. The Iridium network consists of a minimum of 66 active satellites in LEO at an altitude of approximately 781 kilometers, an inclination of approximately 86.4 degrees, and velocities of approximately 27,000 kilometers of hour.

These 66 satellites (plus spares) are strategically positioned to provide voice and data coverage over Earth's entire surface. Each satellite communicates with its neighboring satellite through it K_a band inter-satellite links. Each of the 66 satellites orbit from pole to pole with an orbit of roughly 100 minutes. Each satellite has 48 spot beams arranged as 16 beams in three sectors. Figure 9 shows a depiction Iridium constellation [9].

Figure 9: Iridium Constellation

The Iridium network is capable of communicating both voice and data services. One of the ways to communicate data through Iridium is through a communication protocol called Short Burst Data (SBD). The SBD service currently allows for communication between machine and machine to and from anywhere in the world. The maximum message size is relatively small with a maximum message size able to be sent from a transceiver is approximately 340 bytes. The SDB protocol has a latency of approximately 5 seconds [9].

An example of a transceiver that could potentially be used with the PACS system is the Iridium 9602 modem. Although the equipment to transmit data using SBD is currently available commercial off the shelf (COTS), modifications will need to be made to the 9602 modem to allow it to communicate in space. This modification to the 9602

modem is outside the scope of this thesis but is currently being studied by AFIT with the support of AFRL.

2.10 Variance and Covariance Matrix

This section explains the background on the significance of variances and covariance matrices (CMs). CMs are important to understand in studying conjunction analysis because the CM provides insight into the accuracy level of the position of a RSO. The Conjunction Summary Messages (CSMs) produced by JSpOC provide the CMs for both RSOs involved in the potential collision.

Dr. William E. Wiesel in his book, "Modern Orbit Determination" explains that the positional vector of a RSO does not indicate exactly where the RSO is at a certain instant of time, but instead just the most likely position [10]. However, with the information provided by the corresponding covariance matrix, the statistical certainty of where the RSO is located can be understood.

To describe the covariance matrix, the concepts of variance and covariance will first be described. One of the primary efforts in the field of statistics is attempting to quantify the level of variability of a random variable. The variance parameter is commonly used to define this variability. The variance of a random variable X_i is equal to the expected value of difference between the random variable and its mean. This variance is also equal to the square of the standard deviation σ.

$$Var(X_i) = E\left[(X_i - \overline{X_i}) \right] = \sigma_{X_i}{}^2 \tag{1}$$

While the variance is a measure of the variability of a random vector, the covariance is a measure of the extent to which two variables from two sets of ordered data "move" in the same direction. The covariance of any two random variables (X_i,X_j) is equal to the expected value of the product between the difference of the first variable minus its mean and the second variable minus its mean.

$$Cov(X_i, X_j) = E\left[(X_i - \bar{X}_i)(X_j - \bar{X}_j)\right] \tag{2}$$

Now that the variance and covariance terms have been explained, the CM can be described. In the case of the 3 component position vector, the associated covariance matrix is a 3 x 3 matrix, producing a total of 9 CM elements. In the case of the positional vector of a RSO is in the UVW reference frame, a 3 x 3 covariance matrix is created.

$$CM_{UVW} = \begin{bmatrix} Cov(V_U, V_U) & Cov(V_V, V_U) & Cov(V_W, V_U) \\ Cov(V_U, V_V) & Cov(V_V, V_V) & Cov(V_W, V_V) \\ Cov(V_U, V_W) & Cov(V_V, V_W) & Cov(V_W, V_W) \end{bmatrix} \tag{3}$$

Where:
CM_{UVW} = Covariance Matrix of a vector in the UVW reference frame
V_U = U (Radial) component of vector V
V_V = V (In-Track) component of vector V
V_W = W (Cross Track) component of vector V

The 3 diagonal elements in the matrix CM_{UVW} ([1,1], [2,2], and [3,3]) are the variance of the corresponding V_U, V_V, V_W components. For instance, the first diagonal elemental term [1,1] is the variance of V_U component, which is in the radial component of the positional vector. Additionally the CM is symmetrical (i.e. the matrix element [2,1]

is equal to the matrix element [1,2]). The diagonal terms of the covariance matrix provide the variance (and as a result the square of the standard deviation) of the vector in the corresponding U, V, and W directions.

$$CM_{UVW} = \begin{bmatrix} \sigma_U{}^2 & Cov(V_V, V_U) & Cov(V_W, V_U) \\ Cov(V_U, V_V) & \sigma_V{}^2 & Cov(V_W, V_V) \\ Cov(V_U, V_W) & Cov(V_V, V_W) & \sigma_W{}^2 \end{bmatrix} \quad (4)$$

2.11 Error Ellipsoids

Wiesel explains that the covariance matrix can undergo an eigenanalysis calculation which "will give the principal error axis length and direction in space" [10]. The 1-sigma error ellipsoid (or any scaling of the error ellipsoid) can then be drawn around the position vector. Figure 10 shows a 1 and 3 sigma uncertainty around an object.

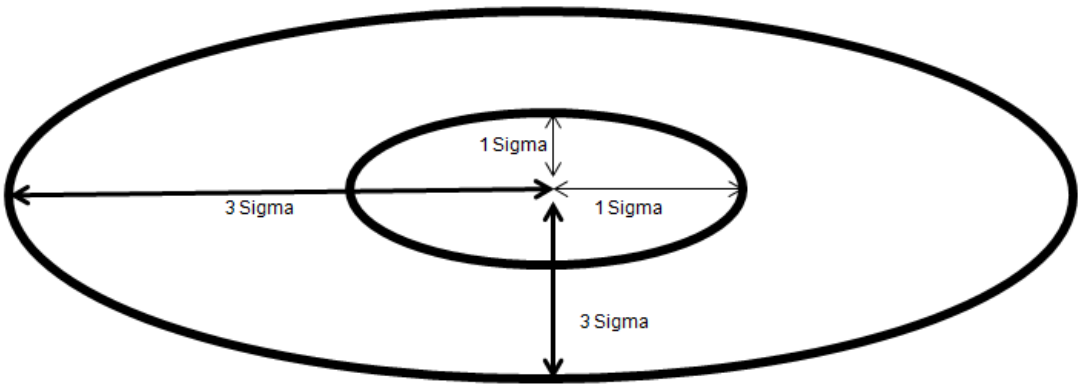

Figure 10: 2-D Representation of a 3-D Error Ellipsoid at 1-Sigma and 3-Sigma (Not to Scale)

Wiesel's text provides the information seen in Table 2 which gives the probability of the RSO being within k-sigma of the projected positional. For example, there is approximately a 20% chance that the object is within 1-sigma of the center. If the error ellipsoid is increased to 3-sigma, then the probably increases to about 97% (or only 3% probability that it is outside the error ellipsoid).

Table 2: Probably of Lying Within a 3 Dimensional Ellipsoid

	1 σ	**2 σ**	**3 σ**	**4 σ**
Probability	0.19872	0.73852	0.97071	0.99887

2.12 Summary

In this chapter, the background information relevant to the PACS system concept of operations and support systems were described. Conjunction analysis and its application at JSpOC were described. Additionally, the covariance matrix and its significance were explained. This background information will support the methodology, results and conclusions in further chapters.

III. Methodology

3 Chapter Overview

This chapter will describe the methodology that was used to complete the research presented in this thesis. First explained are the processes that were used to collect the necessary data for the analysis. In summary, data was collected from two primary sources to perform this analysis: JSpOC supplied data of previous near conjunctions supplied as Conjunction Summary Messages (CSMs); and historic resident space objects (RSOs) data downloaded from the www.beta.space-track.org website. Second, a derivation of the algorithm used to calculate the probability of collision (POC) based solely upon the CSM data is presented. Third, a detailed derivation of the mathematical models used in the modeling and simulation of conjunction analysis is provided. Finally, the overall analysis methodology is described to provide insight into how the accuracy of conjunction analysis would be impacted by the deployment of the PACS system.

3.1 CSM Data from JSpOC

In attempting to quantify the possible improvements of the PACS systems, the first goal was to better understand the "as-is" operations of the current JSpOC system. JSpOC posts orbital inform regarding all of the unclassified RSOs that they track on-line at www.beta.space-track.org. The data provided at this website does not include the necessary covariance matrices that are needed to calculate the POC. Fortunately, the JSpOC stores information on previous near conjunctions as CSMs. Therefore, historic CSM data was requested from JSpOC involving objects in Low-LEO, where Low-LEO is

defined as RSOs with a perigee below 750 km (which is the assumed orbital regime of the PACS system).

3.2 Data – JSpOC Historic Data

A second subsequent ODR was submitted to JSpOC that asked three specific questions regarding conjunctions in 2011 involving RSOs in Low-LEO. These three questions can be seen in Table 3 below. Their respective answers and the significance are described in future chapters.

Table 3: Partial Data from CSM for 10 Conjunctions

1	What was the number of CSMs in 2011 involving satellites in Low-LEO (below 750 km perigee)?
2	Approximate number of unclassified active satellites tracked by JSpOC in 2011 in Low-LEO?
3	Number of JSpOC known collision avoiding maneuvers in 2011?

3.3 Data – Historic Launches

Launch data was collected regarding previous launches of RSOs in order to better model the number of future launches of RSOs that could include a PACS payload. Spreadsheet data was downloaded from an unclassified web-site at www.beta.space-track.org. At this website, registered users are able to access orbital information of most RSOs (excluding classified objects). This website is provided its orbital information from JSpOC [13]. Using this information, the researcher was able to query the number of

historic launches by time period, orbital regime, and object type (i.e., Payload or Rocket Body or Debris).

3.4 Calculating the Probability of Collision from the CSM

This section will discuss the creation of the code created in MATHCAD to calculate the POC. Screen shots of the code written in MATHCAD to calculate the POC can be seen in Appendix 1. Table 4 below provides a summary of certain assumptions used in order to calculate the POC.

Table 4: Assumptions for Calculating the POC [12]

1	Covariance matrix values are accurate.
2	Covariance uncertainty volumes are Gaussian (i.e. Normal).
3	Velocity vector at the time of collision is not subject to uncertainty.
4	Space object sizes are spheres of known radii.
5	Object motion is essentially in a straight line right before the TCA.

Table 5 gives the data necessary from the CSM to calculate the POC. A total of eight values are needed: four from the primary colliding object and four from the secondary object.

Table 5: Data in CSM used in POC Calculations for Both RSOs Involved in the Conjunction

1	3 x 3 Covariance Matrix in UVW Frame (m^2)
2	Velocity Vector in EFG Frame (m/s)
3	Position Vector in EFG Frame (m)
4	Exclusion Volume - in terms of radius (m)

To calculate the POC, it is first necessary to convert the covariance matrices from the UVW frame into the same reference frame as the velocity and position vectors (EFG frame). In the CSMs, the 3x3 covariance matrices for the primary and secondary objects are given in their respective UVW reference frames, while the position and velocity vectors are given in the previously discussed EFG reference frame. Therefore, the transformation matrices to convert the UVW reference frame to the EFG reference frame need to be calculated.

Because the EFG reference frame is not an inertial reference frame, the inertial velocity vectors need to be calculated. The velocity vector takes into account the rotation of the Earth, where the Earth rotates at approximately 7.292E-5 radians per second. The inertial velocity vector can be calculated by using Equation (5).

$$\vec{V_i} = V_{EFG} + R_E \cdot \begin{pmatrix} 0 \\ 0 \\ 1 \end{pmatrix} \times \vec{V}_{EFG} \tag{5}$$

Where:
V_i = Inertial Velocity Vector
V_{EFG} = Velocity Vector in the EFG Reference Frame
R_E = Rotational Rate of the Earth

Once the inertial velocity vectors of the RSOs are calculated, this information can be used to find the coordinate system UVW in terms of the EFG reference frame. The necessary equations to create the UVW reference frame can be seen in Equation (6).

$$U = \frac{\vec{P}}{\left\|\vec{P}\right\|} \qquad W = \frac{\vec{P} \times \vec{V_i}}{\left\|\vec{P} \times \vec{V_i}\right\|} \qquad V = \frac{W \times U}{\left\|W \times U\right\|} \tag{6}$$

Once the U, V, and W components have been found in terms of the EFG reference frame, the next step is to calculate the transformation matrix. Equation (7) shows the transformation matrix that will convert a vector or matrix from the EFG reference frame to the UVW reference frame [14].

$$R_{EFG \to UVW} = \left\lfloor U : V : W \right\rfloor \tag{7}$$

Using the transformation matrix from Equation (7), the covariance matrix in the UVW frame can be transformed to the EFG frame by using Equation (8) [14].

$$CM_{EFG} = R_{UVW \to EFG} \cdot CM_{UVW} \cdot (R_{UVW \to EFG})^T \tag{8}$$

Once the covariance matrices of both the primary and secondary objects are calculated in the EFG frame, the next step is to sum the two covariance matrices. Wiesel explains that covariance matrices (in the same reference frame and units) can be simply added if they are statistically independent. Equation (9) describes this relationship [12].

$$CM_{Combined} = CM_{Asset} + CM_{Debris} \tag{9}$$

The next step in calculating the POC is to create a new coordinate frame with the primary axis along the relative velocity vector. The relative velocity vector is equal to the difference between the asset's velocity and the velocity of the debris as seen in Equation (10). As previously discussed in the section on the CSMs, the first RSO listed is always an active satellite and the other may be any RSO (however, the majority of the time the secondary object is not an active satellite due to high ratio of debris to active satellites in space). Therefore, in this case, the RSO referred to as the "debris" may in fact be an active satellite or any other type of RSO.

$$\vec{V}_{Rel} = \vec{V}_{Asset} - \vec{V}_{Debris} \tag{10}$$

Once the relative velocity vector (V_{Rel}) is calculated, the next step is to normalize it and to compute the other two orthonormal components of this new reference frame. For purposes of this report, this new reference frame is named "RAB." In this new reference frame, the A and B components can be any two vectors that are normalized and

orthogonal to each other and V_{Rel}. Calculating the new A and B components of the RAB reference frame was computed by the Gram-Schmidt process [15].

Once the Gram-Schmidt method is used find the new reference frame, RAB, the combined covariance matrix of the Asset and Debris, $CM_{Combined}$, is converted from the EFG frame to the RAB reference frame. This is performed by calculating the transformation matrix as seen in Equation (11) and using this transformation matrix to compute the CM in the RAB frame as seen in Equation (12).

$$R_{EFG \to RAB} = \left[R : A : B \right]^T \tag{11}$$

$$CM_{RAB} = R_{EFG \to RAB} \cdot CM_{Combined} \cdot (R_{EFG \to RAB})^T \tag{12}$$

The newly created covariance matrix in the RAB frame can be seen in Equation (13).

$$CM_{RAB} = \begin{bmatrix} \sigma_R^{\,2} & Cov(V_A, V_R) & Cov(V_B, V_R) \\ Cov(V_R, V_A) & \sigma_A^{\,2} & Cov(V_B, V_A) \\ Cov(V_R, V_B) & Cov(V_A, V_B) & \sigma_B^{\,2} \end{bmatrix} \tag{13}$$

The miss distance is now calculated between the asset and the debris in the EFG frame by subtracting the position vector of the debris from the asset. Equation 14 below shows the relationship to calculate the miss vector, M_{EFG}.

$$\overrightarrow{M}_{EFG} = \overrightarrow{P}_{A,EFG} - \overrightarrow{P}_{D,EFG} \tag{14}$$

Where:
M_{EFG} = Miss Distance Vector in EFG Reference Frame
$P_{A,EFG}$ = Position Vector of Asset in EFG Reference Frame
$P_{D,EFG}$ = Position Vector of Debris in EFG Reference Frame

Using the EFG to RAB transformation matrix, previously described in Equation 11, the miss distance vector, M_{EFG}, can be converted to the RAB reference frame by using Equation (15).

$$\overrightarrow{M}_{RAB} = R_{EFG \to RAB} \cdot \overrightarrow{M}_{EFG} \tag{15}$$

At this point, both the miss distance vector and the summed covariance matrix are in the 3-dimensional RAB reference frame. Wiesel explains that when calculating the POC the relative velocity vector in the RAB frame is now "irrelevant." [12] By making this assumption, it is now only the "A" and "B" components in the RAB coordinate frame that determine whether the two RSOs collide. Since the relative velocity vector direction is assumed to be irrelevant, a new reference frame can be created derived from the RAB frame where the relative velocity direction is ignored. This new coordinate system is two dimensional, referred to as coordinate system "AB."

The miss distance vector, M_{RAB}, and the combined covariance matrix, CM_{RAB}, now need to be converted to the 2-dimensional AB reference frame. This is simply done

by eliminating the components that contain information regarding the relative velocity component of the RAB frame.

In the case of the 3 x 3 covariance matrix in the RAB frame, by eliminating the relative velocity elements in the RAB covariance matrix the covariance matrix in the AB frame reduces down to a 2 x 2 matrix. This elimination can be seen in Equation (16) below.

$$CM_{AB} = \begin{bmatrix} \cancel{\sigma_R^2} & \cancel{Cov(V_A, V_R)} & \cancel{Cov(V_B, V_R)} \\ \cancel{Cov(V_R, V_A)} & \sigma_A^2 & Cov(V_B, V_A) \\ \cancel{Cov(V_R, V_B)} & Cov(V_A, V_B) & \sigma_B^2 \end{bmatrix} \tag{16}$$

The miss distance vector that is currently in the 3-dimentional M_{RAB} reference frame now needs to be reduced down to the 2-dimensional M_{AB} frame. This is simply done by eliminating the relative velocity vector component, M_R, as seen in Equation (17).

$$\overrightarrow{M}_{AB} = \begin{bmatrix} \cancel{M_R} \\ M_A \\ M_B \end{bmatrix} \tag{17}$$

With the covariance matrices of the asset and debris now in the AB reference frame and the miss-distance in that same AB reference frame, the final step is to calculate the probability of collision. This calculation is performed by calculating a double integral which is a function of the: 1) the summed covariance matrix in the AB frame; 2) the summed exclusion radius of the two objects; 3) and the miss distance between the two

RSOs at the TCA. Equation 18 integrates the two-dimensional area of the circle with radius EV around the origin [12].

$$POC = \frac{1}{2\pi \left| CM_{AB} \right|^{1/2}} \int_{-ER}^{ER} \int_{-\sqrt{ER^2 - B^2}}^{\sqrt{ER^2 - B^2}} e^{\left[-\frac{1}{2} * \begin{bmatrix} M_A - A \\ M_B - B \end{bmatrix}^T * [CM_{AB}]^{-1} * \begin{bmatrix} M_A - A \\ M_B - B \end{bmatrix} \right]} dA dB \tag{18}$$

Where:
ER = Summed Exclusion Radius – summed from the Primary and Secondary RSOs
A = First independent variable
B = Second independent variable
M_A = Projected Miss-Distance in the A direction
M_B = Projected Miss-Distance in the B direction

Upon further discussions with JSpOC, it was discovered that JSpOC calculates a square around the origin with the length of one of the sides as twice the ER (instead of a radius around the origin). Therefore, the actual integrating equation used to calculate the POC is seen in Equation (19) below.

$$POC = \frac{1}{2\pi \left| CM_{AB} \right|^{1/2}} \int_{-ER}^{ER} \int_{-ER}^{ER} e^{\left[-\frac{1}{2} * \begin{bmatrix} M_A - A \\ M_B - B \end{bmatrix}^T * [CM_{AB}]^{-1} * \begin{bmatrix} M_A - A \\ M_B - B \end{bmatrix} \right]} dA dB \tag{19}$$

Figures 11, 12, and 13 depict how the POC is calculated based upon Equation (19). In these graphs, the primary asset is assumed to be centered at the origin and the position of the secondary object is unknown and is statistically based. On these graphs, the most likely position of the secondary object is at the location where the probability

function is at a maximum, in other words, at the "highest point of the graphical mountain." The integration is done over the square at the origin, where one side of the square is two times the radius of the joint exclusion volume. As demonstrated on this graph, the POC can be changed by either changing the projected miss-distance (in other words shifting the location of the peak of the mountain) or by changing the covariance matrix (in other words by changing the shape and/or steepness of the mountain). By decreasing the values of the covariance matrices of either the asset or the debris, the "mountain" becomes steeper as the certainty increases.

To illustrate how the POC changes based upon the covariance matrices and the miss distance, Figures 11, 12, and 13 show 3 examples where the relative size of the covariance matrices and the miss-distances are manipulated.

First, Figure 11 shows a conjunction where the summed covariance matrix values are very low (accuracy is very high) and the projected miss-distance is approximated to be zero. To calculate the POC, the area inside the exclusion square (depicted as a dashed square on the graphs) is integrated. In Figure 11 it can be seen the POC approaches 1 (almost 100% certain there will be a collision) since nearly all of the probability density function (PDF) is enclosed in by the exclusion square.

In contrast, Figure 12 shows a conjunction where the summed covariance matrix values are much larger and the estimated miss-distance is still zero. In this example, the POC is not nearly as high since a large portion of the PDF is not encapsulated by the exclusion square.

Finally, Figure 13 represents a conjunction where the summed covariance matrix is very small but the miss-distance is large by comparison. In this example, the POC is approaching 0 since nearly none of the PDF is encapsulated by the exclusion square. As illustrated in the graphs below, the ideal situation in determining whether a conjunction will occur is when the summed covariance matrix is very small and the miss distance is either very small (a POC approaching 1 as seen in Figure 11) or very large (a POC approaching 0 as seen in Figure 13).

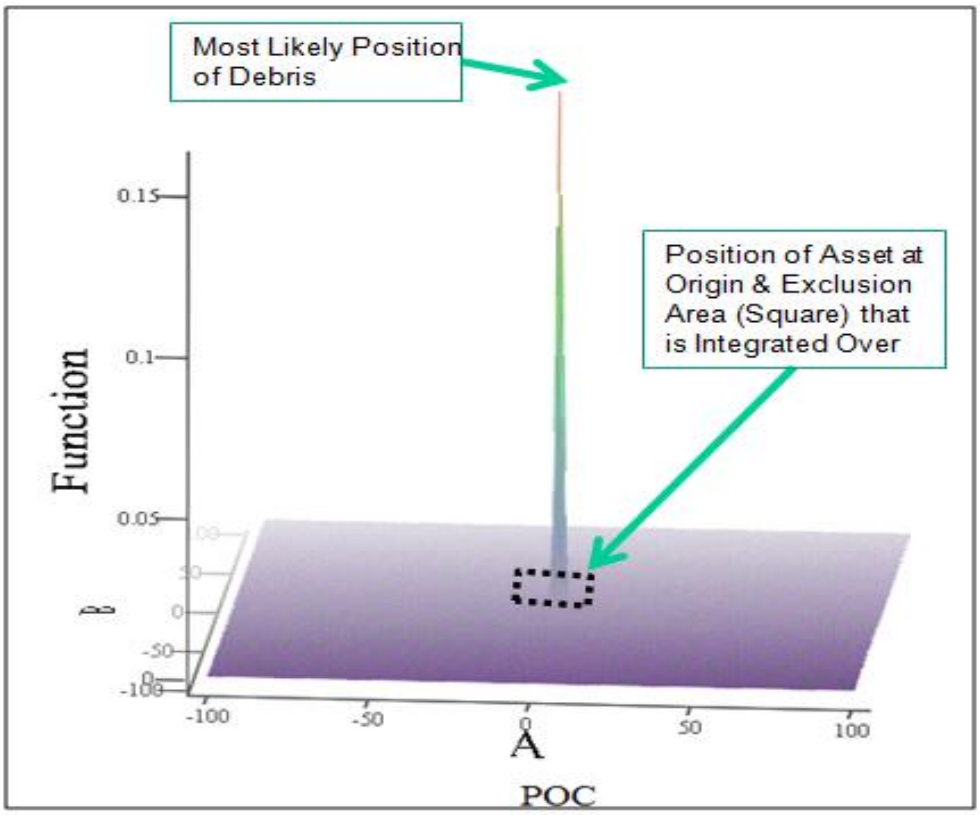

Figure 11: Graph of Calculating POC in MATHCAD where the Summed Covariance Matrix is Relatively Small and the Projected Miss Distance is Zero. Here the POC Approaches 1.

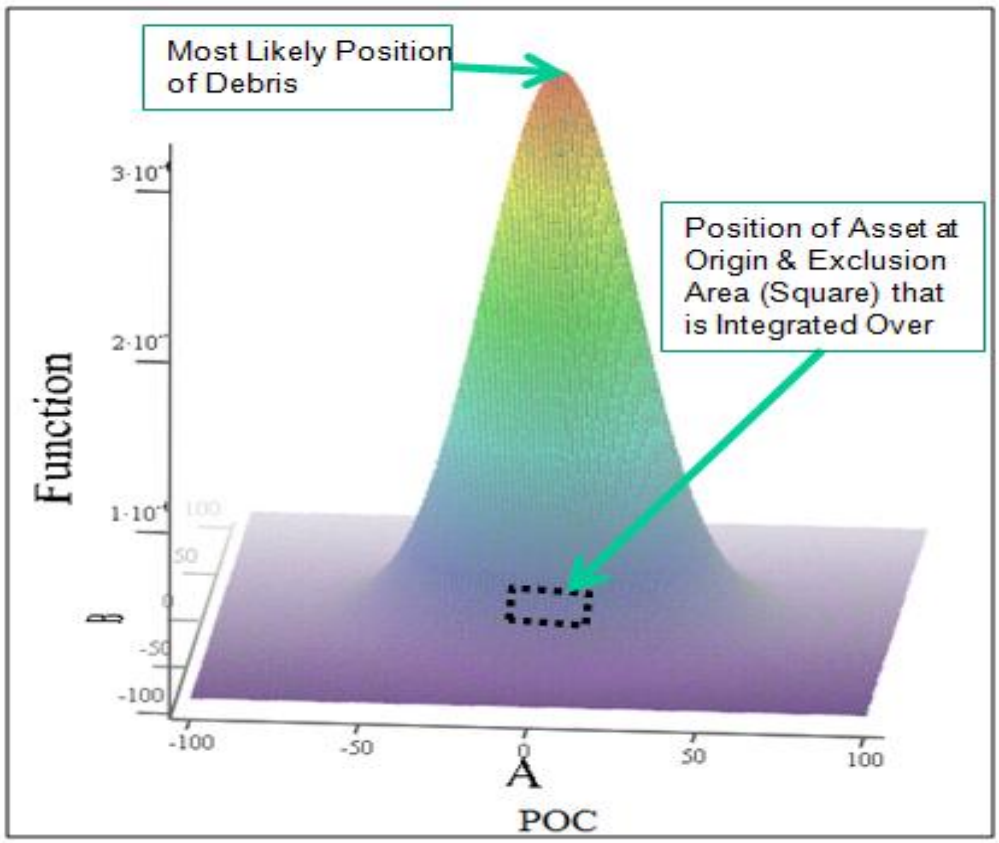

Figure 12: Graph of Calculating POC in MathCAD where the Summed Covariance Matrix is Relatively Large and the Projected Miss Distance is Zero. Here the POC is Somewhere Between 0 and 1.

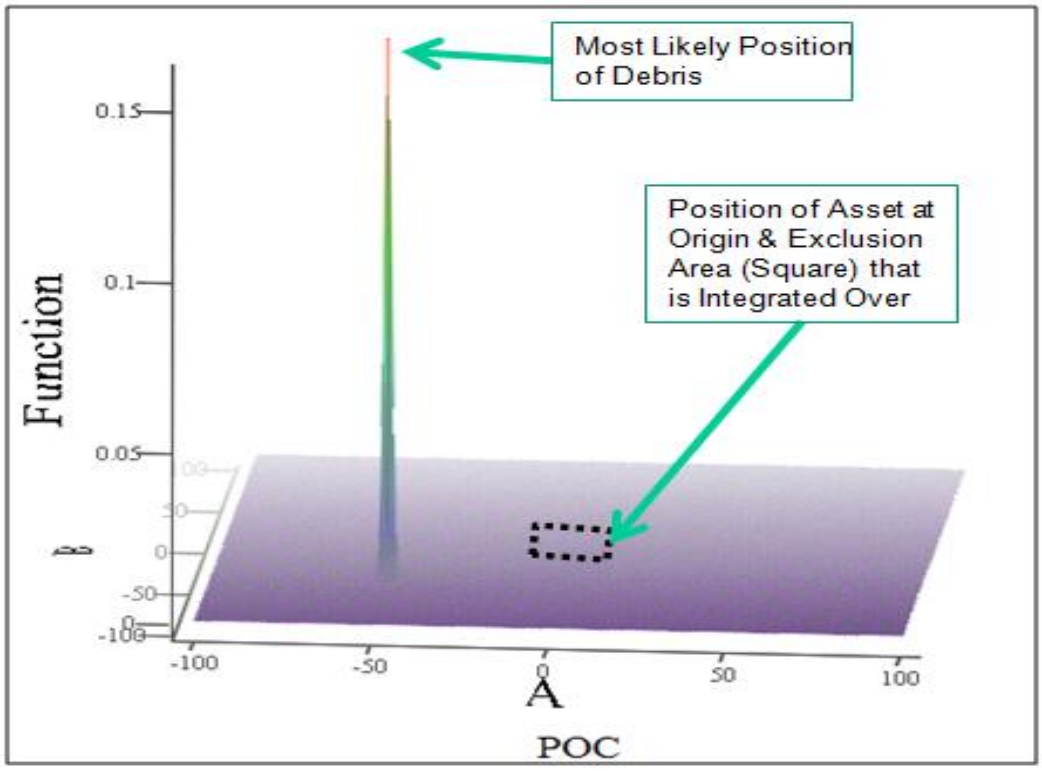

Figure 13: Graph of Calculating POC in MATHCAD where the Summed Covariance Matrix is Relatively Small and the Projected Miss Distance is Relatively Large. Here the POC Approaches 0.

3.5 Estimating the Covariance Matrices for the PACS Payload

In order to model the potential improvement of the PACS system to conjunction analysis it was necessary to estimate the accuracy capabilities of a future PACS payload. This estimation was necessary in order to model the impacts of having the PACS payload on either of the two RSOs involved in the conjunction.

Since the PACS payload is pre-operational, no data was readily available to effectively quantify the orbital determination capabilities of the system. Therefore, it was necessary to estimate the accuracy capabilities the system might have. Making this

estimation was difficult because there were several unknown variables that must be taken into account to estimate the covariance matrix of a RSO. A partial list of these unknown factors is listed in Table 6 (in no particular order).

Table 6: PACS Operational Use Variables

	Undetermined Operational Variable of the PACS System	**Significance**
1	How often does the PACS Payload collect data from GPS and how often is that data transmitted back to JSpOC?	Increasing the collect and transmit rate would decrease the covariance size.
2	What is the orbit of the RSO?	RSOs in different orbits will have varying error growth propagation rates.
3	How much time is there between epoch and the time of closest approach?	Error propagation growth is a function of time.
4	Accuracy level of GPS receiver on the PACS Payload?	Accuracy is dependent upon the GPS receiver equipment and the GPS mode used.

Since the specifics on the operational variables of the PACS system are largely yet to be determined, the expected precision of the PACS payload is largely unknown and needs to be estimated. In order to best represent the future capabilities of the PACS system, it was decided that an optimistic and conservative estimate would be used. These two values from this point on would be referred to as "PACS-Small" (or PACS-S) and "PACS-Large" (or PACS-L), where PACS-S is the smaller and more optimistic covariance matrix and PACS-L is the larger and more conservative estimate. It is anticipated that as this system develops and evolves the system capabilities will be better defined. However, for the purposes of this analysis the PACS-S and PACS-L approach will be used.

The first step to estimate the covariance matrix sizes of PACS-S and PACS-L was to research the capabilities of space based GPS receivers. For example, there is a GPS receiver built by the Novatel corporation called the OEMV-1G receiver. According to Novatel's specification sheet, the performance accuracy, in terms of root mean square (RMS), which is largely analogous to the standard deviation, is 1.5 meters [16]. Therefore, at time epoch, (assuming no propagation error) the PACS payload could, in theory, be accurate to better than the 1.5 meter level (1-sigma level). Accordingly, the PACS-S (optimistic estimate) covariance matrix was chosen, for purposes of this model, to have a 1-sigma radius of 1 meter. Additionally, it was assumed that the covariance values in the non-diagonal terms of the covariance matrix were zero. The covariance matrix of PACS-S was can be seen in Equation 20. Additionally, an illustration of PACS-S can be seen in Figure 14.

$$PACS-S=\begin{bmatrix} 1^2 & 0 & 0 \\ 0 & 1^2 & 0 \\ 0 & 0 & 1^2 \end{bmatrix} \tag{20}$$

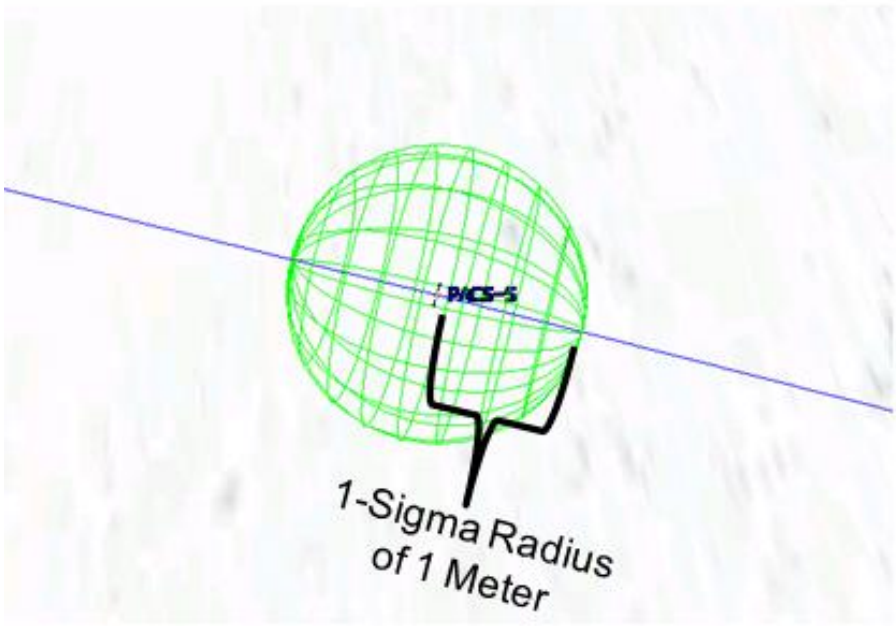

Figure 14: STK Screen Shot of PACS-S with a 1-Sigma Radius of 1 Meter

Next, the PACS-L, which is meant to be the more conservative estimate of the accuracy of the PACS capabilities, was assumed to be a sphere similar to the PACS-S except that PACS-L has a 1-sigma radius of 10 meters. The covariance matrix for PACS-L can be seen in Equation 21. Additionally, an illustration of PACS-L can be seen in Figure 15.

$$PACS-L=\begin{bmatrix} 10^2 & 0 & 0 \\ 0 & 10^2 & 0 \\ 0 & 0 & 10^2 \end{bmatrix} \tag{21}$$

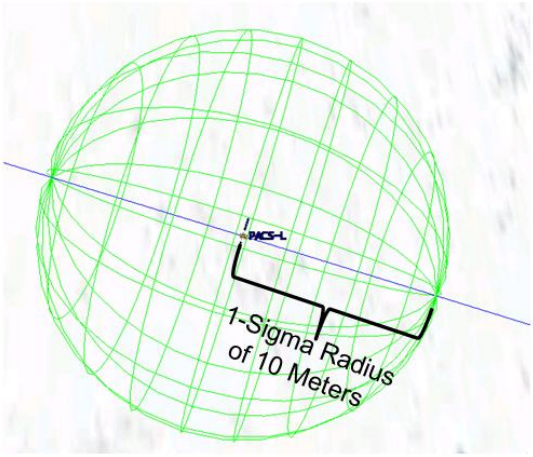

Figure 15: STK Screen Shot of PACS-L with a 1-Sigma Radius of 10 Meters

3.6 Modeling the Incorporation of the PACS System on Historical Conjunctions

Now that statistical accuracy level of the PACS payload had been estimated as PACS-S and PACS-L, the next step in the methodology was to change the covariance matrix of either the primary or secondary object to the PACS-S or PACS-L level, and subsequently re-calculating the POC.

For the purpose of the model for this thesis, ten distinct scenarios were created and their corresponding POCs were calculated. Five of which were where the conjunction had the original miss distance and five were where the miss distance was decreased to zero. The results of these calculations of the POCs for these 10 scenarios can be seen in subsequent chapters.

Table 7: 10 Scenarios to Model the Impact of PACS

Scenario	Original Projected Miss-Distance	Scenario	Projected Miss-Distance of "0"
1	Original CMs	6	Original CMs
2	PACS-L on Asset	7	PACS-L on Asset
3	PACS-L on Debris	8	PACS-L on Debris
4	PACS-S on Asset	9	PACS-S on Asset
5	PACS-S on Debris	10	PACS-S on Debris

3.7 Modeling the Number of RSOs that Could Incorporate a PACS Payload

One of the primary questions involving the PACS system is the number of RSOs that could potentially incorporate a PACS payload. It was decided to evaluate the number of PACS enabled objects could be in orbit after a ten year period after the system goes operational. In order to make this estimation, two primary assumptions regarding PACS need to be made. These assumptions are identified in Table 8 below.

Table 8: 2 Assumptions for Incorporating PACS Payloads to RSOs

1. PACS payloads can only be placed on RSOs that have not yet launched. This is assuming that it would be cost prohibitive to put PACS payloads on RSOs already in orbit.
2. PACS payload can only be placed on RSOs that will have a perigee below 750 km. This particular altitude is identified because it is assumed that the RSO will need to be at an altitude lower than the Iridium constellation (which is at approximately 781 km)

In order to estimate the number of RSOs that can be launched in the future, the number of launches in the recent past first needs to be estimated. The www.beta.space-

track.org website has a search function that allows an authorized user to download information regarding previous launches, their country of ownership and the type of object.

To first estimate the number of launches in the future, the number of launches that had occurred in the previous five years was searched (e.g., 2007- 2011) for launches into Low-LEO. This information was used to develop a mathematical model to estimate future Low-LEO launches. In addition to the total number of launches, the object type, and launch country was calculated.

To estimate the number of PACS enabled RSOs, the amount of time that these objects will remain in orbit also need to be estimated. For example, if within the first year of operations for the PACS system, 20 RSOs are enabled with PACS, but 50% of these RSOs re-orbit within 2 years, then obviously only 10 of these original PACS enabled RSOs are still on orbit and assisting JSpOC with the conjunction analysis mission 2 years in the future. In order to estimate the length of on-orbit time for potential PACS enabled RSOs, the previous 5 year time period was insufficient. Therefore, the launches of rocket bodies in the 1990s (1 January 1990 to 31 December 1999) were evaluated and their time on orbit was evaluated.

3.8 Summary

This section has provided information on the methodology for this thesis. The process to obtain data on historic conjunctions from JSpOC was explained. Subsequently, the steps to research historic launches from www.beta.space-track.org were described. The process of calculating the POCs was also explained. As well as the

methodology used to estimate the number of potential PACS payload that could be launched in the future.

IV. Results

4 Chapter Overview

This chapter will provide the results that follow the methodology described in the previous chapter. First discussed are the PACS systems architecture views. Next, this chapter will include a section that shows the results of modeling the impacts of the PACS payloads to the POCs. Additionally, a section will include the results of modeling the number of potential PACS payload that could become operational. Finally, a section will include the results of the study of the number of collisions that typically occur to RSOs in Low-LEO.

4.1 PACS Systems Architecture

This section of the results section contains the high level system architectures for the PACS system. Figure 16 shows the Operational View 1 (OV-1). Shown in this OV-1 are the major support systems involved in the operational use of the PACS system. This view and its significance were described in previous chapter.

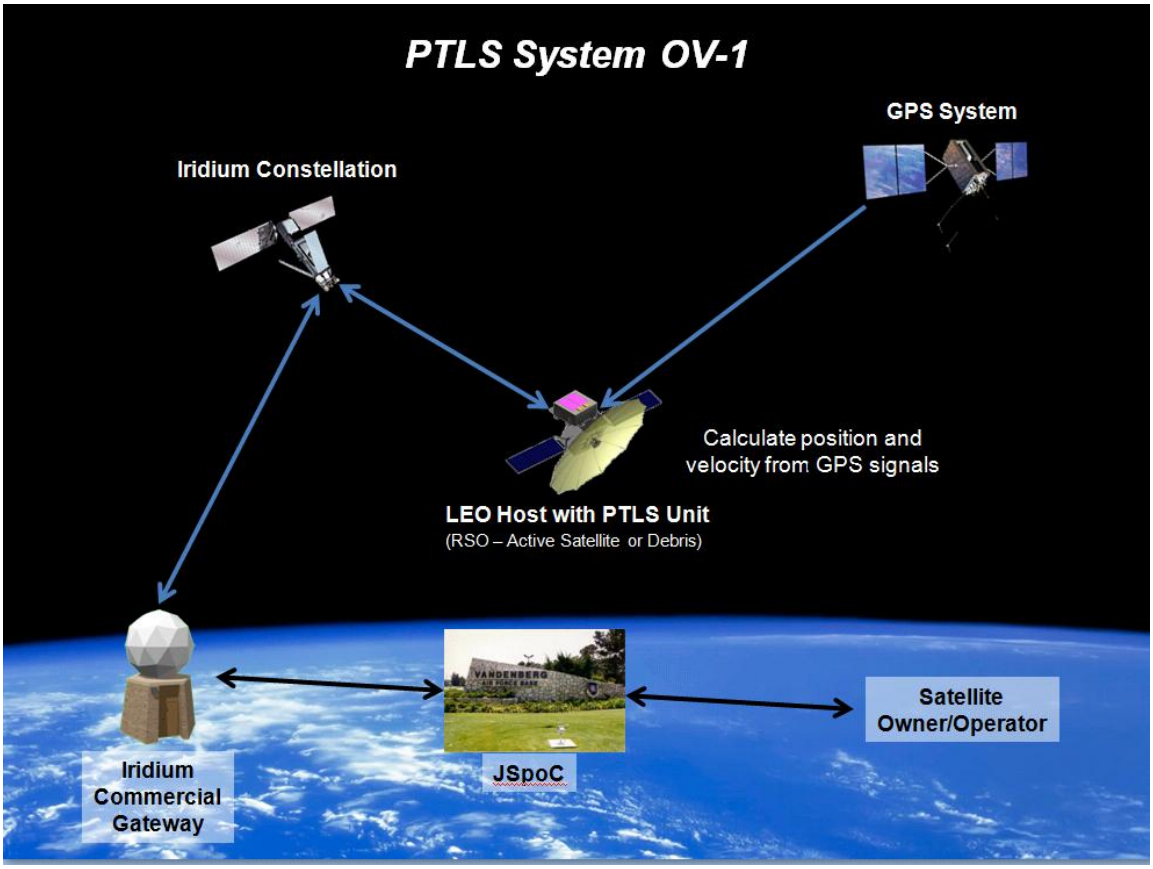

Figure 16: Operational View 1 (OV-1) – High-Level Operational Concept Graphic

The second DoDAF architecture view created was the Operation View -2 (OV-2) as seen in Figure 17. This view provides a description of the flow of resources between the various operational activities. In this OV-2, the resources are the data being sent to and from the following systems: 1) GPS Satellite Constellation; 2) PACS Payload; 3) Iridium Communication Network; 4) JSpOC; 5) Satellite Owner/Operator.

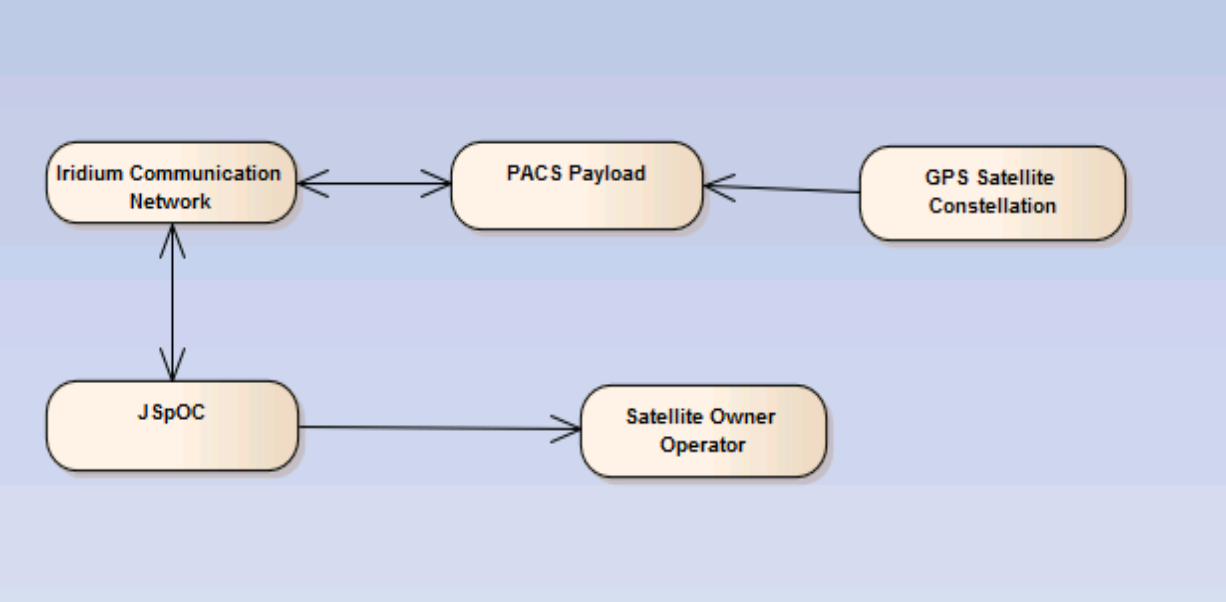

Figure 17: Operation View 2 (OV-2) – Operational Resource Flow Description

The next diagram created was the OV-5a, which is the Operational Activity Decomposition Tree. This view shows the operational activities organized in a hierarchal structure. As seen in Figure 18, the primary activity was defined as "Provide RSO Orbital Information to JSpOC." In order to accomplish this primary activity of the PACS system several sub-activities need to be accomplished. These activities include: 1) Compute RSO Orbital Information; 2) Receive Transmissions; 3) Send Transmissions; 4) Power Management; 5) Command and Data Management. These 5 sub-activities also have their respective sub-activities. Obviously, as the PACS system is better defined this view will likely change and expand to include additional sub-activities.

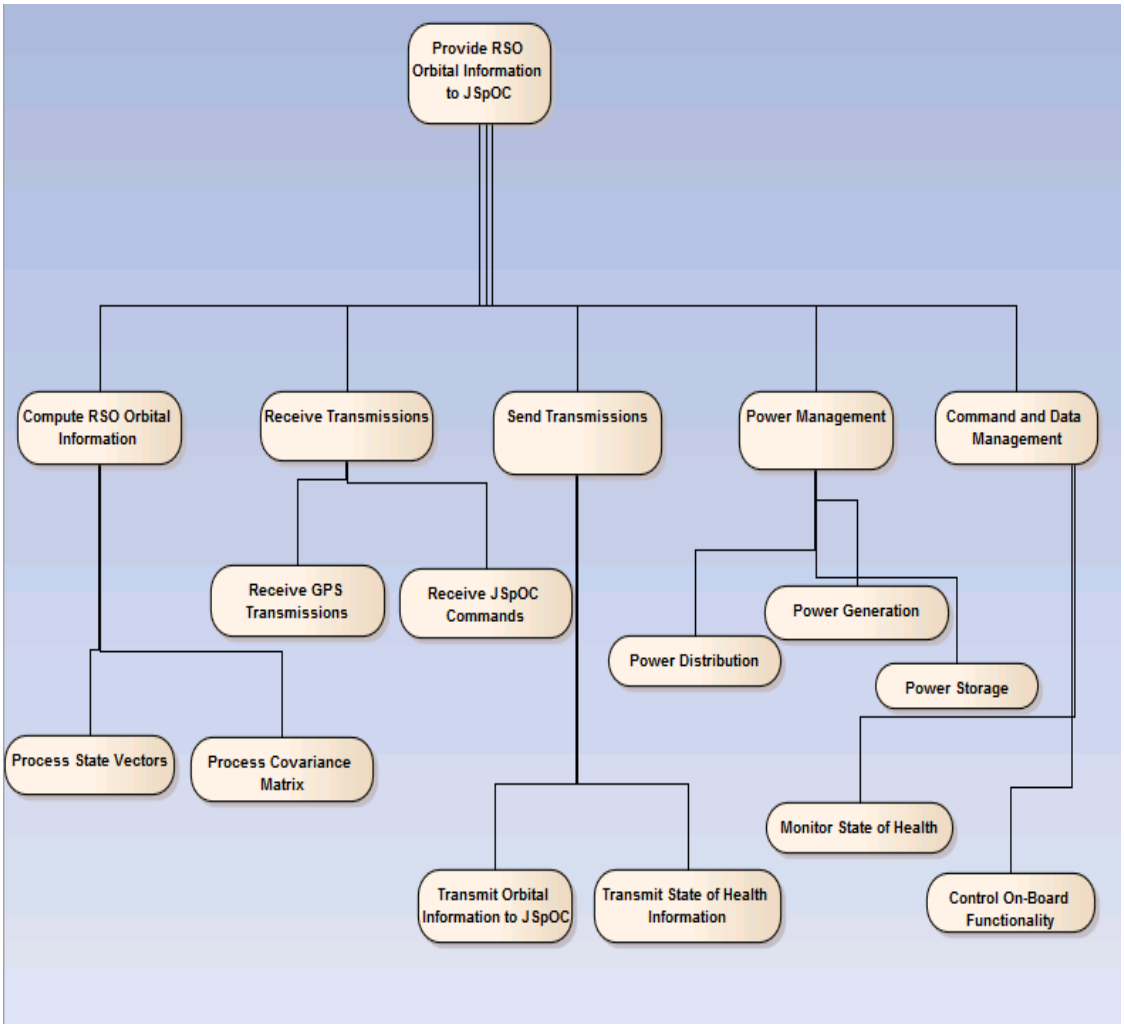

Figure 18: Operational View 5a (OV-5a) – Operational Activity Decomposition Tree

The final DoDAF product created was the Operation View 6c (OV-6c). This view is known as an "Event-Trace Description." This architecture view traces the necessary actions of a given operation scenario. Two OV-6c were created for two separate scenarios. The first diagram (seen in Figure 19) was for the operational scenario where the PACS payload provides the orbital information back to JSpOC on a set regular basis. This is referred to as the Periodic Case. For example, in the Periodic Case the

PACS payload will transmit the orbital information back to JSpOC on a set frequency (i.e., once a minute, or once an hour, or once a day, etc.). In contrast, the second scenario is the On-Demand Case (seen as Figure 20). In this scenario, the PACS payload will only transmit the orbital information back to JSpOC only when a request is made by JSpOC. For example, JSpOC might request an orbital update if a potential conjunction is identified. Because the operational concept of the PACS system is largely yet to be determined, these operational views are likely to evolve.

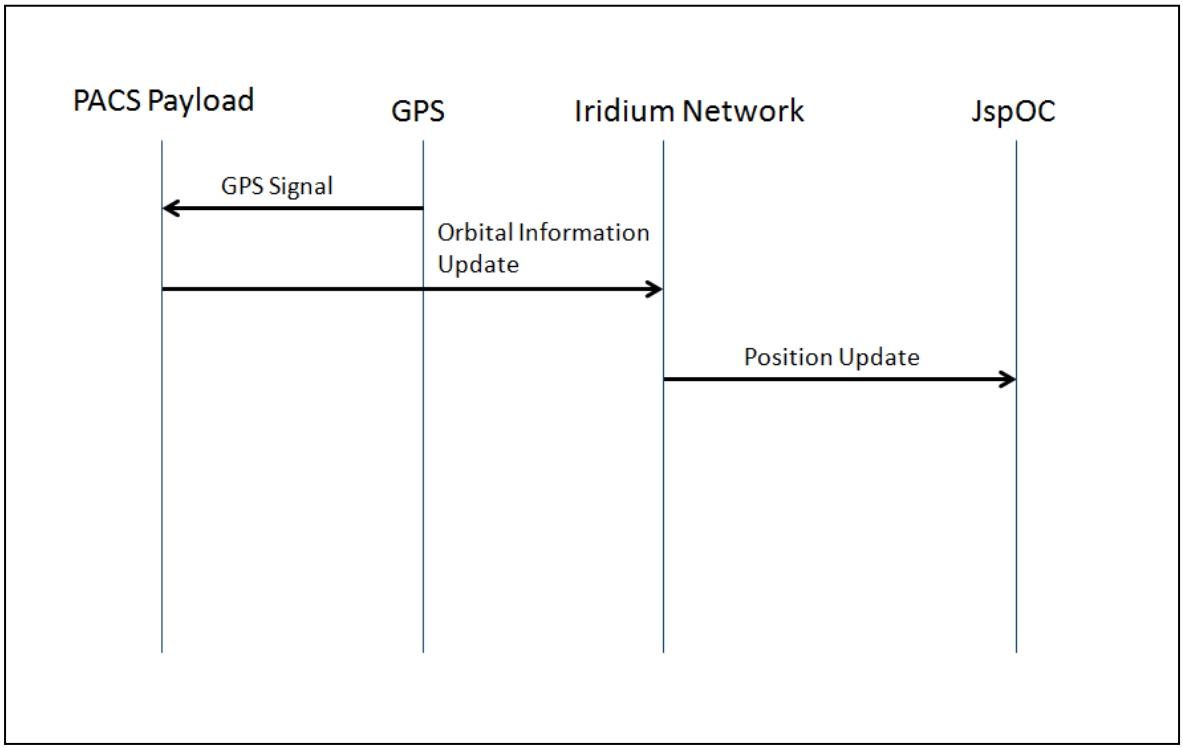

Figure 19: Operational View 6c (OV-6c) - Periodic Case

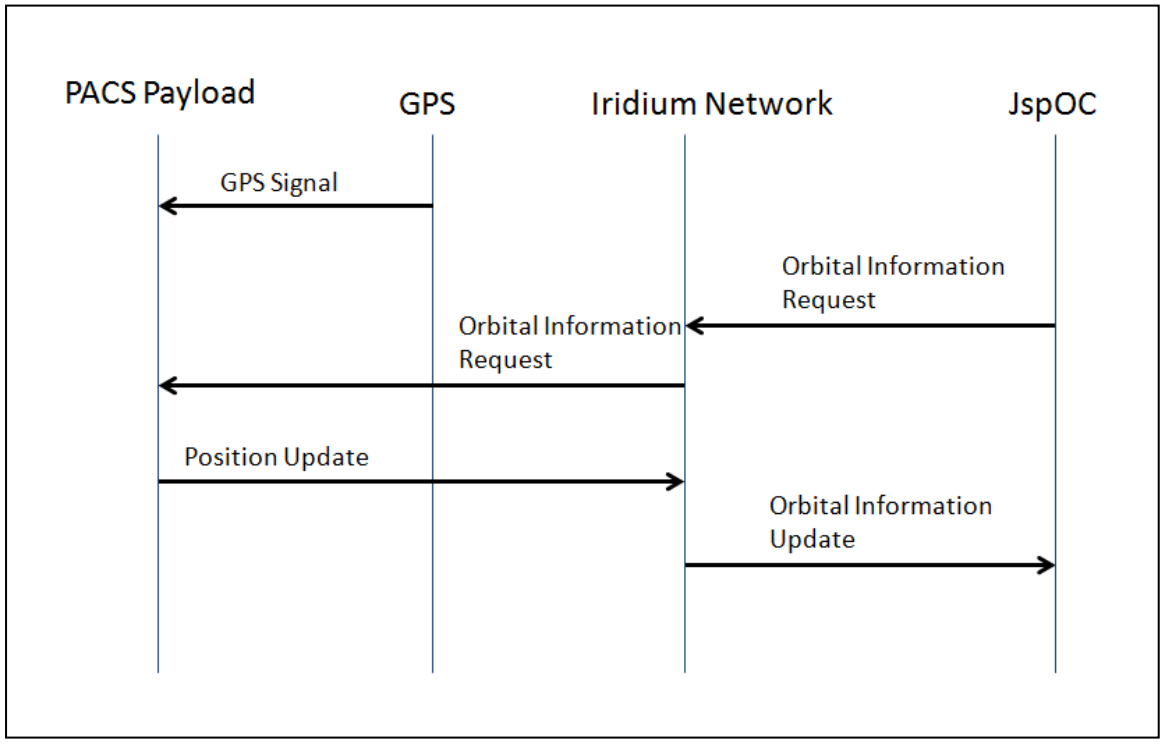

Figure 20: Operational View 6c (OV-6c) – On-Demand Case

These operational DoDAF views provide a basic operational vision of the PACS system. However, as the system is better defined the operational views will likely need to be update to reflect the evolved vision of the developing system. Additionally, a more complete DoDAF architecture will need to be developed which will include the other viewpoints that were previously discussed.

4.2 CSM Data Received from JSpOC

The data source to estimate the impact of the PACS system to conjunction analysis was the CSMs provided by JSpOC. Once the 15 CSMs were delivered it was determined that 10 of the 15 had a time until conjunction of approximately 24 hours or less. The other 5 conjunctions had times until conjunction of 30 to 72 hours. These five

conjunctions were excluded from this study in order to analyze conjunctions that are as similar to each other as possible. The shortest time until conjunction of the 10 conjunctions used in this analysis was approximately 1 hour and the longest time until conjunction was approximately 26 hours. The projected miss-distances ranged from 57 meters to 1203 meters.

Table 9 below provides basic information of the 10 conjunctions used in this study (in no particular order). These 10 conjunctions all occurred between the month of May and October of 2012.

Table 9: Partial Data from CSM for 10 Conjunctions

Conjunction Number	Time Until Conjunction (hrs)	Projected Miss-Distance (m)
1	21.45	199
2	23.31	370
3	2.80	699
4	9.24	879
5	14.54	829
6	6.96	57
7	7.19	376
8	26.16	1,203
9	0.89	588
10	24.98	258

4.3 Calculating POCs in the CSM

Once the necessary code was created in MATHCAD (as explained in Chapter 3), the POC was calculated for each of the 10 conjunctions. This was done in order to compare the algorithm created in MATHCAD to the POC values supplied by JSpOC for

these conjunctions. The results can be seen in Table 10. In the second column are the POCs provided by JSpOC, and in the third column are the POCs calculated by using the method described in this chapter. In all ten of the cases, the error calculated between the supplied values and the calculated values was less than 10%. The source of the difference was never determined. However, for this analysis it was decided that an accuracy error of less than 10% was sufficient for the model. The created MathCAD code can be seen in Appendix 1.

Table 10: POC Calculations and Error for the 10 JSpOC Supplied Conjunctions

Conjunction Number	POC-JSpOC Calculated	POC-MathCAD Calculated	Error
1	2.27E-04	2.27E-04	0.02%
2	0.00E+00	0.00E+00	0.00%
3	0.00E+00	0.00E+00	0.00%
4	1.48E-04	1.48E-04	0.01%
5	6.33E-08	6.34E-08	-0.12%
6	0.00E+00	0.00E+00	0.00%
7	1.38E-19	1.34E-19	3.01%
8	4.17E-07	4.16E-07	0.02%
9	6.37E-06	6.38E-06	-0.13%
10	2.48E-11	2.72E-11	-8.80%

Now that the necessary algorithm to calculate the POC based solely upon data provided in the CSM was created and validated, the researchers had the capability to change the covariance matrix of either the primary or secondary object to the PACS-S or PACS-L size, and subsequently re-calculating the POC.

4.4 As-Is Tracking Capabilities of JspOC Based Upon 10 CSMs

To model the improvements that the PACS system might provide to conjunction analysis, JSpOC's current capabilities were analyzed. This analysis was based upon the

data from the 10 CSM's provided by JSpOC. Listed below in Table 11 are the CSM data that shows the 1-sigma uncertainty for the 10 conjunctions in the UVW reference frame (radial, in-track, cross-track). These values were computed by taking the square root of the diagonal terms of the covariance matrices as described in Chapter 3.

Table 11: 1-Sigma Uncertainty in the UVW Frame (Radial x In-Track x Cross-Track)

Conjunction Number	Primary Object (1-Sigma)	Secondary Object (UVW 1-Sigma)
1	33m x 295m x 19m	210m x 12743m x 70m
2	8m x 58m x 8m	10m x 38m x 5m
3	3m x 32m x 5m	24m x 218m x 18m
4	20m x 90m x 13m	374m x 1376m x 1618m
5	19m x 100m x 10m	69m x 1373m x 45m
6	1m x 8m x 1m	2m x 15m x 5m
7	6m x 18m x 3m	37m x 229m x 18m
8	11m x 58m x 5m	66m x 4936m x 40m
9	9m x 47m x 7m	50m x 357m x 104m
10	12m x 481m x 11m	7m x 38m x 5m

In all 20 of the involved RSOs the largest uncertainty is in the in-track direction. For example, in Conjunction #1, the primary object has an uncertainty of approximately 33 meters in the Radial direction, 295 in the In-Track direction, and 19 meters in the Cross-Track direction. Therefore, the ratio of the uncertainty in the In-Track direction to the uncertainty in the Radial direction or the Cross-Track direction is approximately 10-to-1 (295 meters divided by 33 meters or 19 meters). For the majority of the following analysis, the 1-sigma uncertainty In-Track will be used as the primary metric to quantify the uncertainty of tracking a particular RSO. Figure 21 shows the 1-sigma In-Track uncertainty as a function of the time until the conjunction for all 20 RSOs.

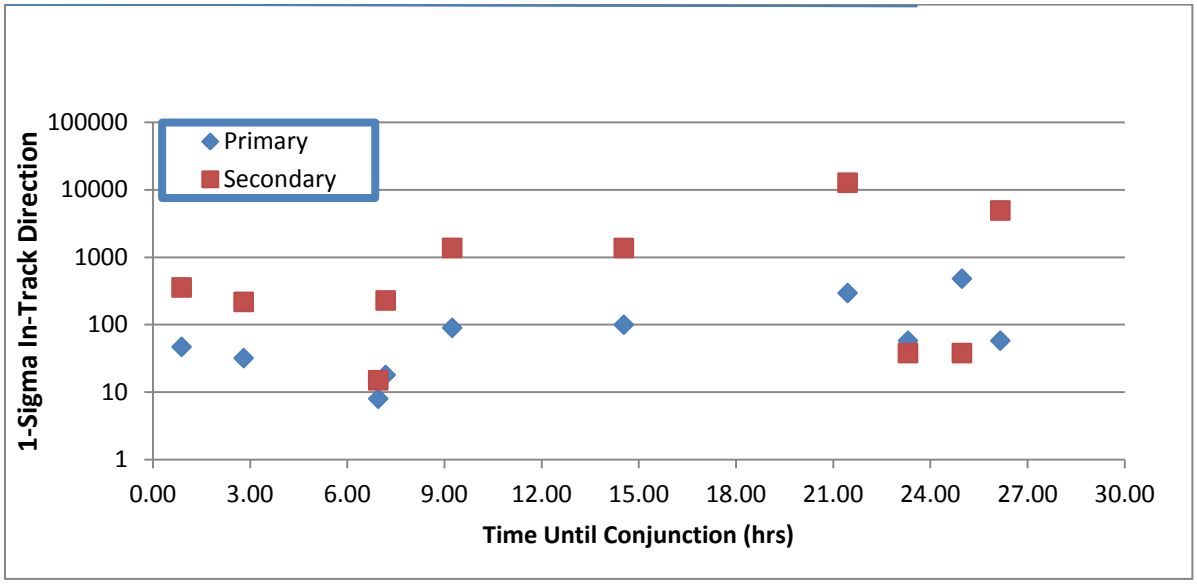

Figure 21: In-Track Uncertainty as a Function of Time Until the Conjunction

The median value for the 1-sigma In-Track uncertainty for the 10 primary objects is approximately 58 meters, with a corresponding standard deviation of 151 meters. The equivalent value for the 10 secondary objects is 293 meters, with a corresponding standard deviation of 4017 meters. For the 10 conjunctions, the primary objects (which are always active satellites) have a smaller uncertainty than the secondary objects (which are typically some type of debris) in 8 of the 10 conjunctions. Figure 22 shows the ratio of the in-track uncertainty of the secondary RSO to that of the primary RSO.

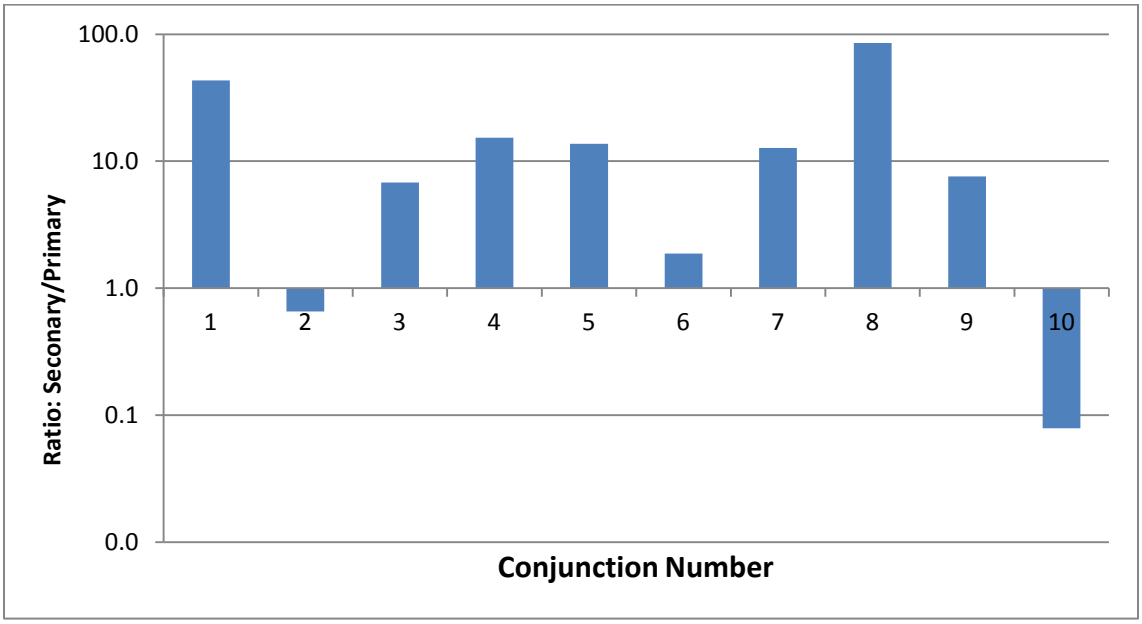

Figure 22: Ratio Between the 1-Sigma Uncertainty in the In-Track Direction of the Secondary to the Primary Objects

From the small data set of these 10 conjunctions, it is clear that on average the primary objects are typically tracked better than the secondary objects.

4.5 JSpOC Tracking Data

Included in the CSM data provided by JSpOC are the data of the tracking frequency for the RSOs. This frequency represents the average number of times per day that a RSO is observed via the SSN over the previous days. This tracking frequency had a large variance, where the frequency varied from as infrequent as approximately 0.7 times per day to approximately 49.7 times per day. In Figure 23, the average number of tracks per day is plotted against the 1-sigma uncertainty in the in-track direction.

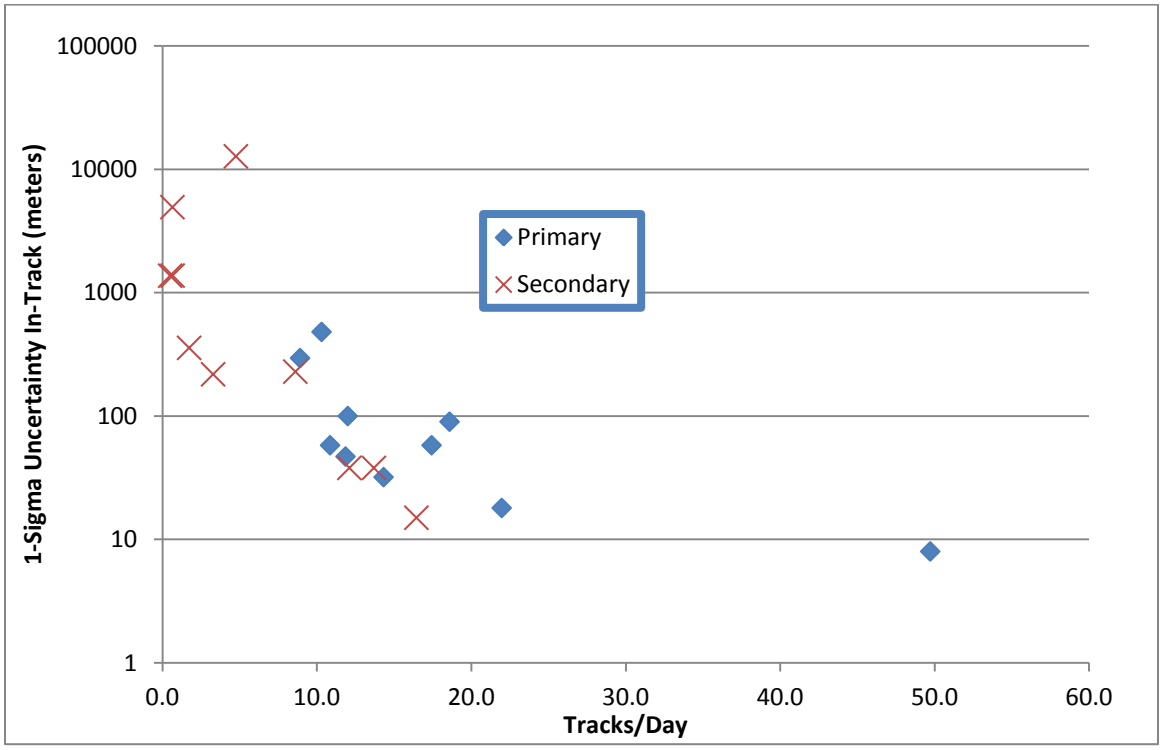

Figure 23: 1-Sigma Uncertainty In-Track vs Number of Tracks per Day

As seen in Figure 23, the objects with the most uncertainty are also the objects that are the least seldom tracked. The best tracked RSO (with an approximate 8 meter 1-sigma uncertainty in the in-track direction) is also the RSO that is tracked the most often (approximately 49.7 tracks per day). Figure 24 shows the frequency that the RSOs are tracked by conjunction number. As seen in this figure, the primary object is tracked more frequently than the secondary object in 9 out of the 10 conjunctions (with the 10th conjunction being the exception).

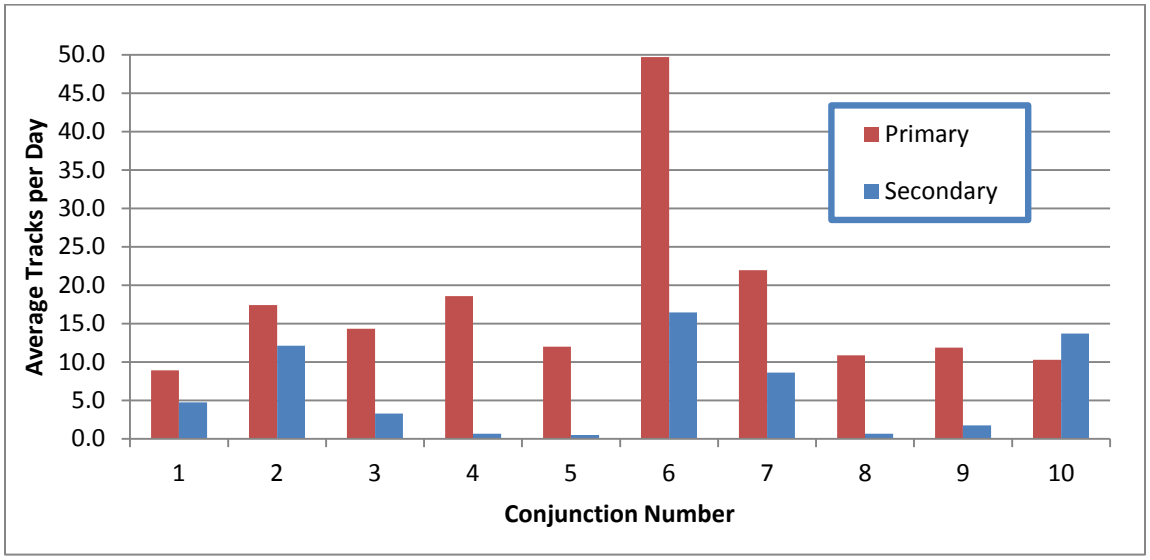

Figure 24: Comparing the Average Tracks per Day for Primary and Secondary Objects

Figure 25 further represents this track frequency data. As seen in this figure, all primary objects are tracked at least 5 times per day on average, where 6 of the 10 secondary objects are tracked less than 5 times per day.

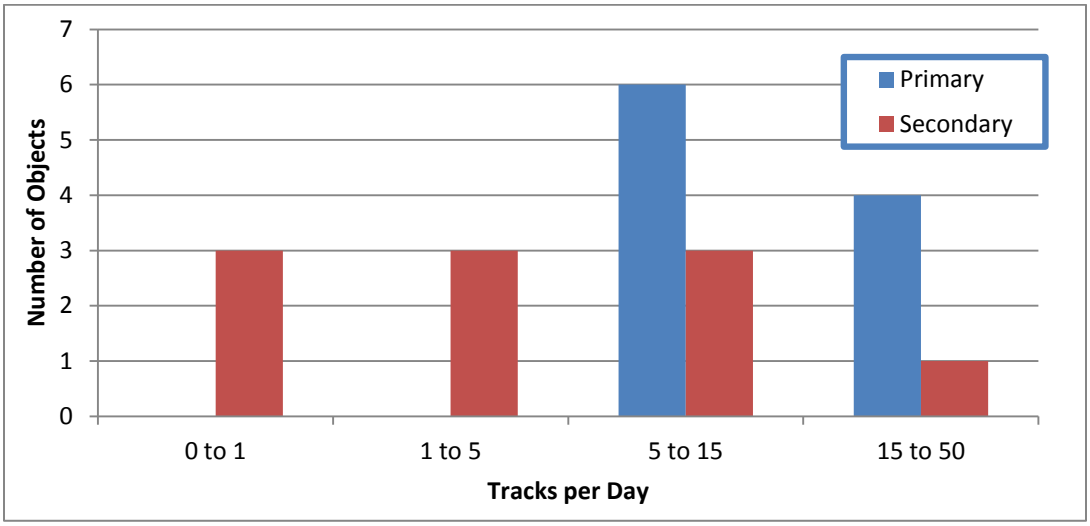

Figure 25: Average Tracks per Day for Primary and Secondary Objects

Based upon this sample set, currently JSpOC tracks primary objects (active satellites) more often than secondary objects (which are typically debris). The primary objects have a median frequency of approximately 17.6 tracks per day, where the secondary objects have a median frequency of approximately 6.2 tracks per day.

4.6 Modeling the Probability of Collision for Conjunction #9

In order to illustrate the impact of changing the covariance matrix on either the primary or secondary RSO calculations were first performed on one of the ten conjunctions, specifically the 9th conjunction. This 9th conjunction, like all of the other 9 conjunctions, involved an active satellite conjuncting with a piece of space debris. The projected miss-distance was approximately 588 meters and the time until closest approach was approximately 1 hour. The 1-sigma in-track uncertainty of the debris and asset were 47 meters and 357 meters, respectively. To model the impacts of PACS, first the POC was calculated assuming neither of the two RSOs had a PACS payload. Subsequently, the POC was recalculated assuming that either the primary or secondary objects either a PACS-S or PACS-L covariance matrices (4 modeling scenarios). Finally, a calculation was made for the scenario where both the primary and secondary objects had either the PACS-S or PACS-L covariance matrices. In this scenario, the calculated probability of collision is reduced as the certainty of the position of the objects increases.

As an illustration of the process of changing the covariance of an RSO, Figure 26 shows a STK screen shot of Conjunction #9 at the time of closest approach. Figure 26 shows the original 1-sigma covariance matrices for both the primary and secondary objects (assuming that PACS has not been incorporated). Note that the primary object,

which is an active satellite, is represented by the yellow color and the debris is in red. Also notice that the debris has a much larger error ellipsoid in comparison to the error ellipsoid of the asset. In this scenario, the original POC (without the inclusion of the PACS payload) was calculated to be 6.37E-6, or roughly a 1 in 157,000 chance of collision.

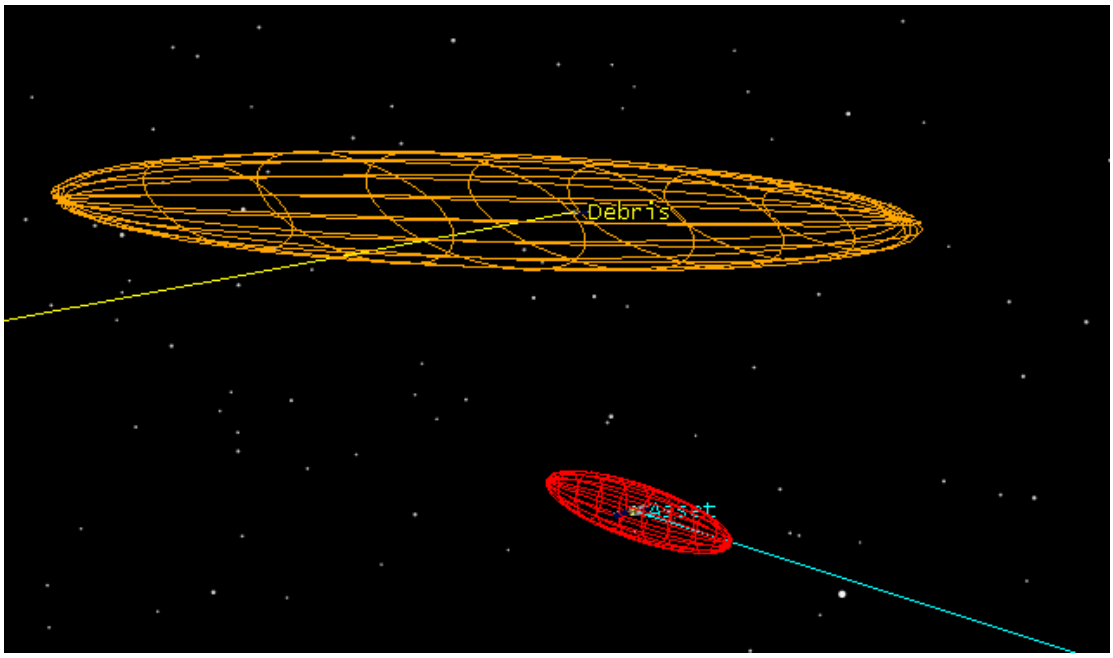

Figure 26: Conjunction #9, Assuming No PACS on Either Object

Figure 27 represents this same conjunction with the exception that the debris incorporated the PACS-L covariance matrix size. It is assumed that all other variables stay constant. For example, the position and velocity vectors of both objects stay the same. Notice that the error ellipsoid drawn around the debris (in yellow) shrinks dramatically. With the inclusion of the PACS payload, the probability of collision decreases to approximately 6.0E-50, which is approaching a POC of 0 (in fact, according

to the CSM data provided by JSpOC, when JSpOC calculates the POC, if the POC is below 1E-20, the value is reported as 0).

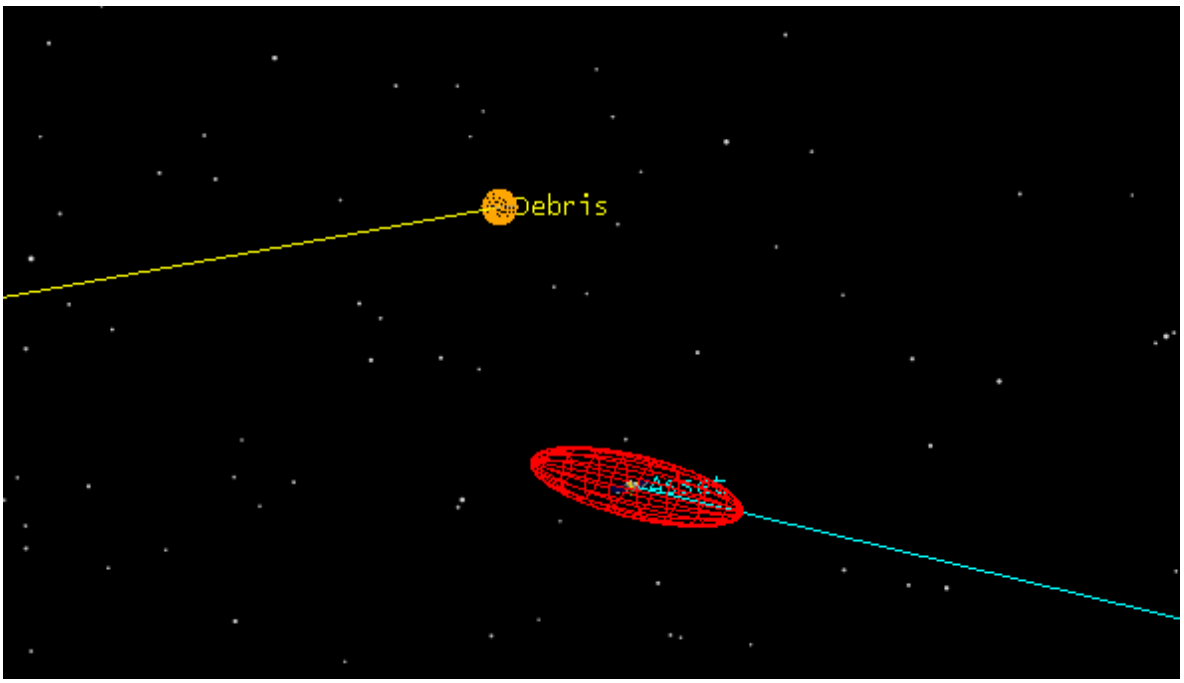

Figure 27: Conjunction #9, Assuming PACS-L on the Debris

Figure 28 shows the same Conjunction #9, with the exception that the Covariance Matrix of the Asset has been reduced to the size of the PACS-L. Here the POC changes to approximately 5.33E-6, or approximately 1-in-188,000.

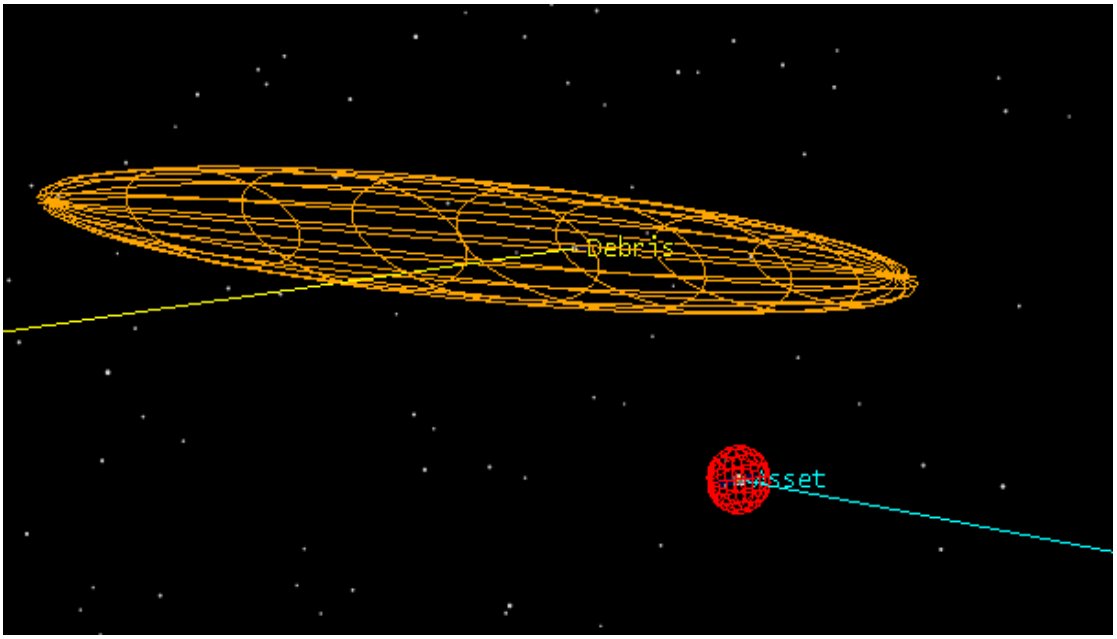

Figure 28: Conjunction #9, Assuming PACS-L on the Asset

In the case of Conjunction #9, the POC (which was originally approximately 6.37E-6) changed dramatically when the assumption was made that the PACS payload (PACS-L) was on the debris (6.0E-50). However, this change in POC was not nearly as dramatic when the assumption was made that the PACS (PACS-L) payload was on the asset (5.33E-6).

Figure 29 shows this change in probability of collision based upon the scenario. Note that the dependent variable scale is the logarithm of probability of collision to the negative one power. On this scale, a value of 3 is equivalent to a POC of 0.001 (1E-3 or 1 in 1000); a value of 5 is equivalent to a POC of 0.00001 (1E-5 or 1 in 100,000); a value of 20 is equivalent to a POC of 1E-20. As seen in the figure, the original POC (before the inclusion of the PACS covariance matrices) is approximately 6.38E-6 (or approximately 1 in 157,000). If it is assumed that the covariance matrix of the secondary

objects is reduced to the PACS-L size, then the POC is decreased dramatically to approximately 6E-50 (Note that JSpOC presents a POC of '0' whenever the calculated POC is smaller than 1E-20). However, if instead, the primary object substitutes the CM of the PACS-L, the POC does not change nearly as dramatically (to 5.33E-6 or approximately 1 in 188,000). Additionally on the graph are the calculations assuming the inclusion of the CM for the PACS-S. The POC values are labeled next to their respective data points.

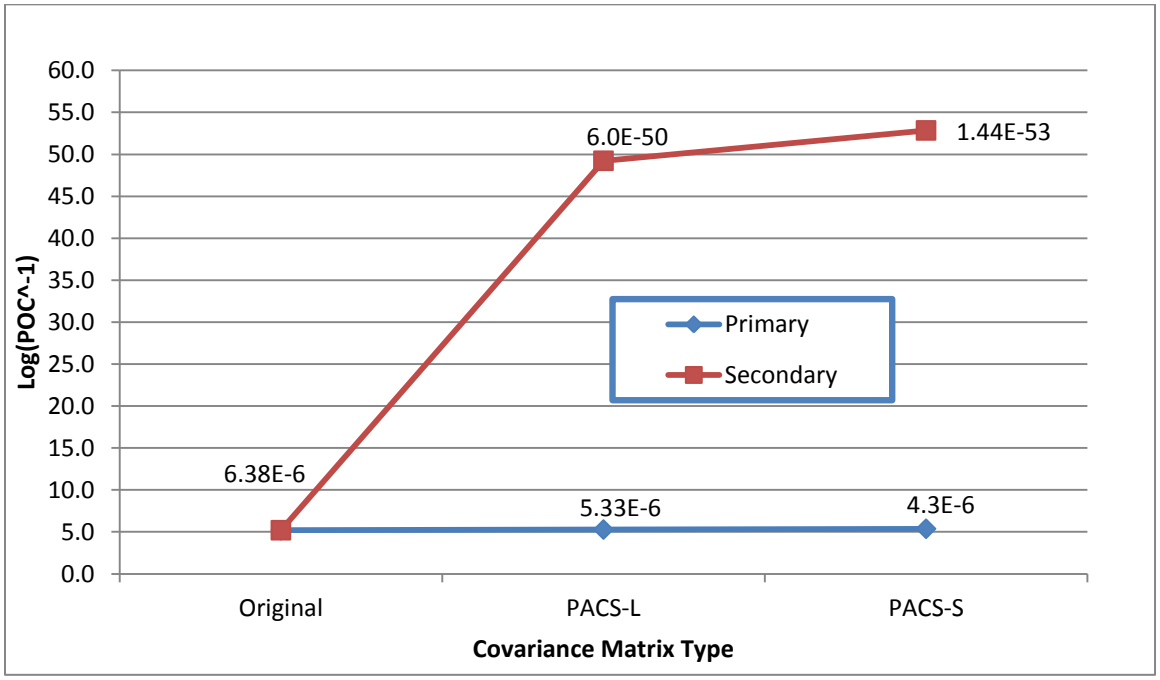

Figure 29: Modeling the 9th Conjunction Assuming the Inclusion of PACS-S or PACS-L

Figure 29 shows that in this scenario, the inclusion of the PACS CM on either of the RSOs produces a decrease in the POC. However, the POC is most dramatically

changed when the PACS CM is substituted on the secondary object (the debris). The change to the POC is relatively minimal when substituted on the primary object.

As seen in Figure 29, as the modeled CM size is decreased the POC decreases. However, if the projected miss-distance is very small, then as the certainty of the position of the objects increases, then the POC should increase. To demonstrate this point, the 9th conjunction is reevaluated assuming a projected miss-distance of 0 meters. This assumption of a 0 miss-distance does not mean that a collision is necessarily certain. For example, with the original CM sizes and a projected miss-distance of '0', the POC is approximately 0.0022 (or roughly 1 in 455). In other words, even if the two RSO are projecting to have a '0' miss-distance, there is still only an estimated 1 in 455 chance that there will be a collision. However, if the uncertainty of the object's position at time of collision is approaching '0' and there is a projected miss-distance is also '0', then the POC will approach 1. Figure 30 shows the same modeling data as shown in Figure 29, with the exception that the projected miss-distance is assumed to be 0. Notice that in this graph is also included the scenario where both of the RSOs have PACS payloads.

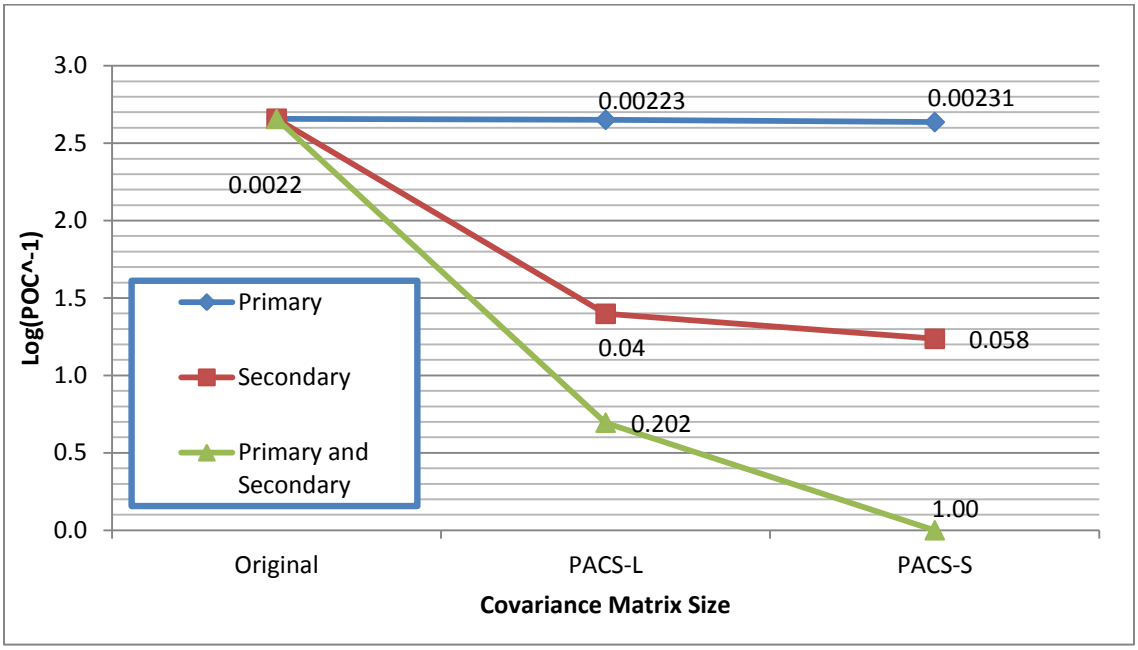

Figure 30: Modeling the 9th Conjunction Assuming the Inclusion of PACS-S or PACS-L and a Project Miss Distance of '0'

As seen in Figure 30, in all three scenarios the POC increases as the covariance matrix size decreases. Again, the most dramatic change to the POC occurs when the PACS payload are assumed to be on the secondary objects. For example, the POC changes from an original 0.0022 (or approximately 1 in 455) to 0.04 (or approximately 1 in 25) when the secondary CM value is substituted with the PACS-L CM. When both objects included the PACS-L the POC increases to 0.202 and when both objects included the PACS-S the POC approaches '1' (or %100).

In this conjunction #9 example, the POC changes dramatically when the PACS payload is assumed to be on the secondary object. The change is not nearly as significant when the assumption is that the PACS payloads are on the primary object. This is because in this scenario, the original CM of the secondary object was much larger than

that of the primary object. By decreasing the uncertainty of the RSO with the largest original CM the largest impact is made to the calculation of the POC.

4.7 Results of the POC Modeling for the 10 Historic Conjunctions

In the previous section the impacts of including the PACS payloads were shown for the 9th conjunction. In this section, all 10 conjunctions are evaluated in a similar fashion and a summary of the results are presented.

In Figure 31, a summary of the results to the POC are displayed for each of the 10 conjunctions. For each of the 10 conjunctions, there were a total of 5 POC calculations where the projected miss-distance was assumed to stay constant: 1) The original CMs, assuming that there were no PACS payloads; 2) PACS-L on the primary object; 3) PACS-S on the primary object; 4) PACS-L on the secondary object; 5) PACS-S on the secondary object.

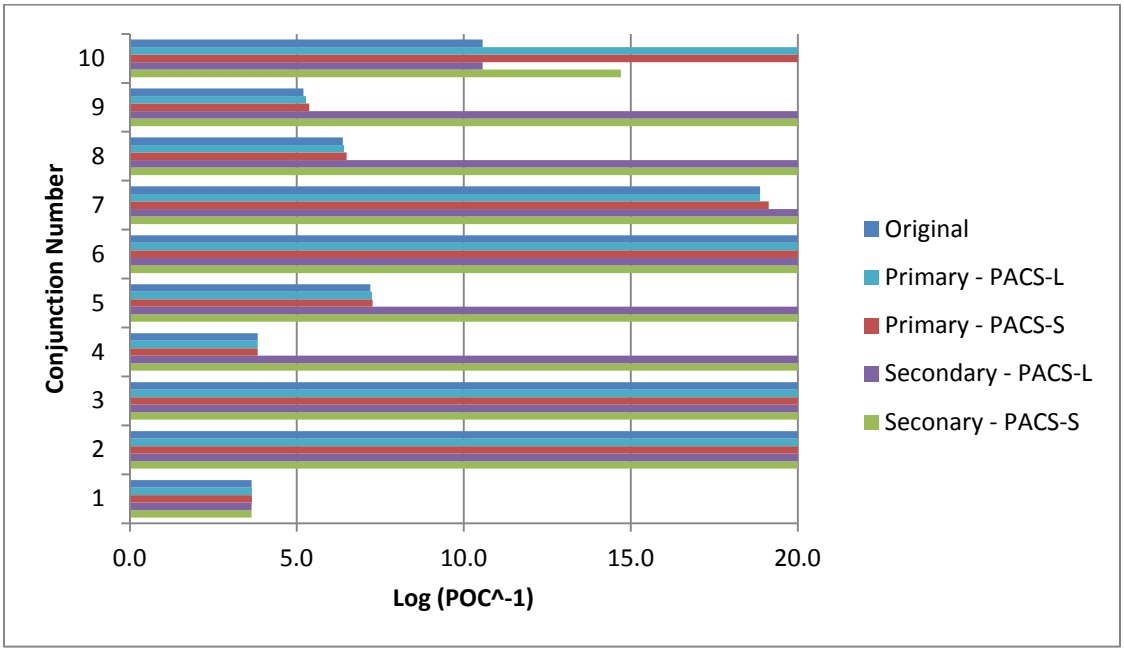

Figure 31: Modeled Changes to the POC for the 10 Historic Conjunctions

This process was repeated where the projected miss-distance is assumed to be '0' in all 10 cases. The corresponding graph can be seen in Figure 32.

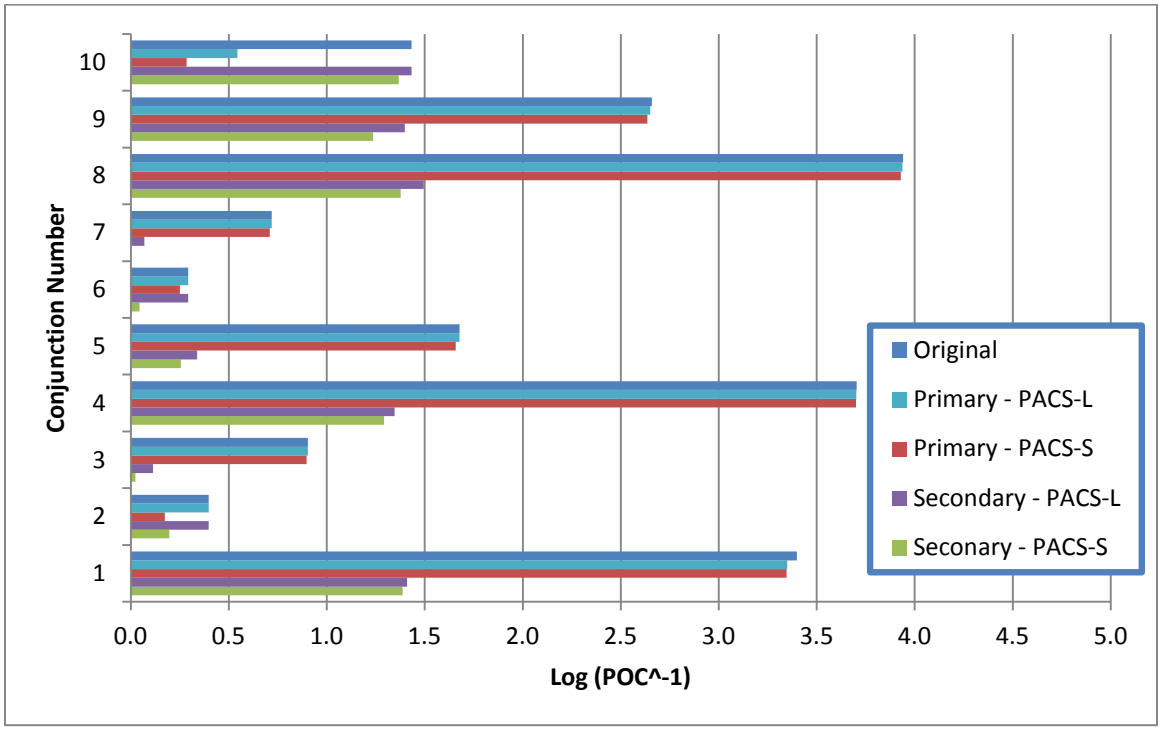

Figure 32: Modeled Changes to the POC for the 10 Historic Conjunctions (Assuming a '0' Miss-Distance)

To summarize these results, additional graphs were produced the conjunctions were sorted based upon their POCs. Three categories were organized: 1) Original CM, assuming no PACS payloads; 2) Primary – PACS (S or L), assuming that there is either a PACS-S or PACS-L payload on the primary object; 3) Secondary – PACS (S or L), assuming that there is either a PACS-S or PACS-L payload on the secondary object. Four separate 'POC Bins' were identified: 1) POC higher than 0.01; 2) POC between 0.01 and 1E-5; 3) POC between 1E-5 to 1E-20; 4) POC lower than 1E-20.

Figure 33 represents the case where the projected miss-distance is assumed to be constant. Originally there were two conjunctions where the POC was greater than 1E-5. That number did not change if the PACS payload was assumed to on the primary object.

However, if the PACS payload is assumed to be on the secondary object, the number decreases to one.

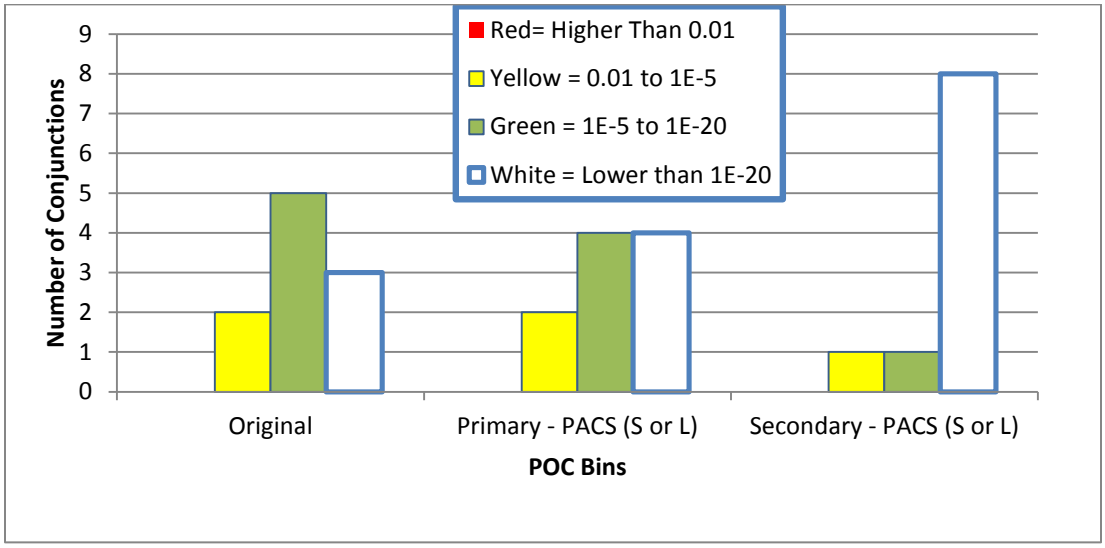

Figure 33: POCs with Original Projected Miss-Distance

Figure 34 shows this same graph for the case where the projected miss distance is '0'.

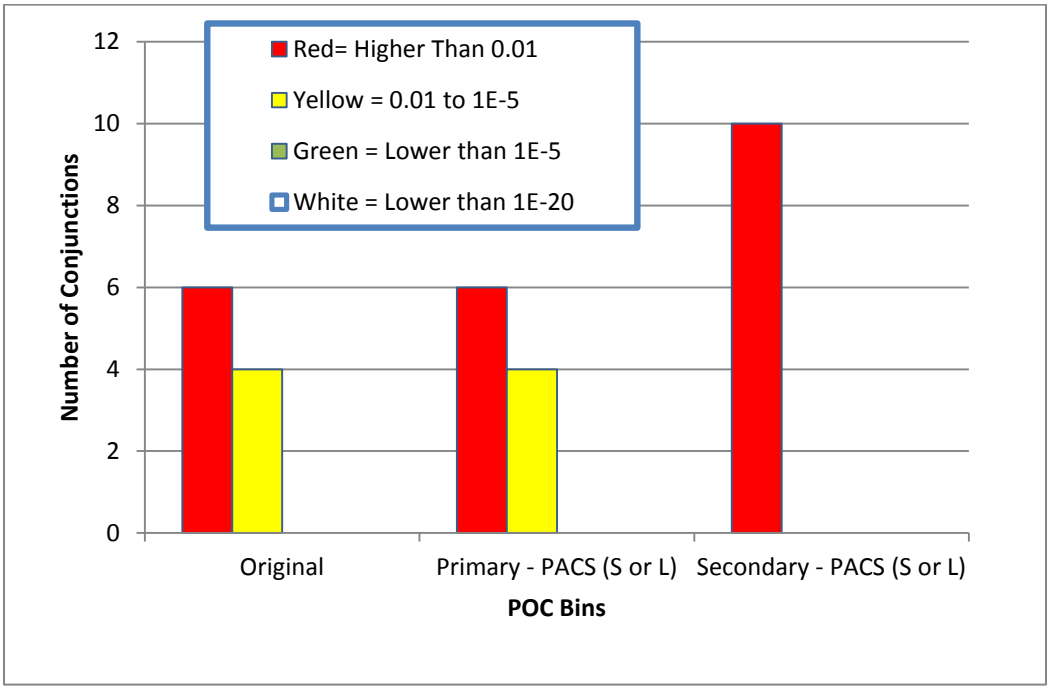

Figure 34: POC with Original Projected Miss-Distance

Notice in Figure 34, that there were originally 6 conjunctions where the POC was higher than 0.01. If the primary object is assumed to have a PACS payload, then that number stays constant. However, if the secondary object had the PACS payload then all 10 objects will have a POC over 0.01.

To further summarize the impact of having a PACS payload hosted on a RSO, the results were studied to determine how often the inclusion of the PACS payload (PACS-S or PACS-L) had a significant impact on the original conjunction. For the purposes of this study, a two significant digit change (either 100 times more or 0.01 times less) in the POC was deemed a significant impact. For example, it is estimated that in the 10 historic conjunctions if the debris had a PACS-S payload then a significant impact would have been made to the POC 9 out of 10 of the conjunctions (90%).

Table 12: Number of Conjunctions Where PACS had a Significant Impact
(Change of Two Significant Digits)

Modeling Scenario	Percentage Significantly Impacted
Asset with PACS-S	30% (3/10)
Asset with PACS-L	10% (1/10)
Debris with PACS-S	90% (9/10)
Debris with PACS-L	90% (9/10)

Therefore, if the conservative estimation of the capabilities of PACS is made (PACS-L), then it is estimated that the PACS payload will make a significant difference to the conjunction 90% of the time for the debris and 10% of the time for the asset.

4.8 Estimating the Number of Potential PACS Enabled Objects

This section of the paper will attempt to analyze the number of potential RSOs that could in the future have on it a PACS payload. The time period chosen was 10 years after the program becomes operational. In order to make this estimate, several assumptions will need to be made. First, that only RSO that can incorporate a PACS payload are those that have not yet launched and therefore can have the PACS payload attached to it prior to launch. The second assumption is that PACS will only go on objects that will have a perigee below 750 km. Third, that PACS will only go on non-active objects (classified as either rocket bodies or debris). By using these assumptions an estimate of the number of PACS enabled RSO will be made.

The first step in estimating the number of objects that could potentially have a PACS payload was to estimate the number of objects that are launched into Low-LEO each year. Figure 35 shows the total number of objects that were launched into Low-

LEO (perigee below 750 km). For example, in 2011 there were a total of 177 objects launched into Low-LEO across the world. This includes all object types, including rocket bodies, payloads, and debris. Obviously, not all of these objects are still on orbit. For example, as of 15 November 2012 (when the data for this analysis was collected), 107 of these 177 objects were still on orbit, meaning that 70 of these objects had decayed.

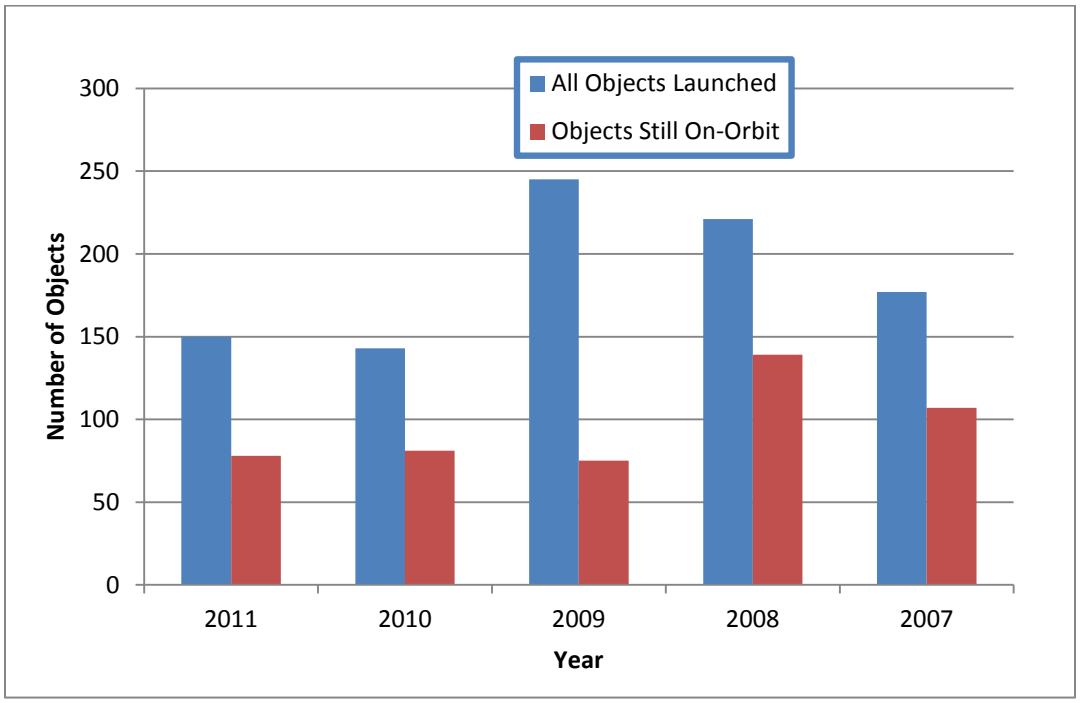

Figure 35: Objects Launched in Orbit by Year into Low-LEO

Based upon these last 5 years, the average number of objects launched into Low-LEO is approximately 187. This includes payloads (active satellites), rocket bodies, and debris. Figure 36 shows the number of objects launched into orbit by year and by object type.

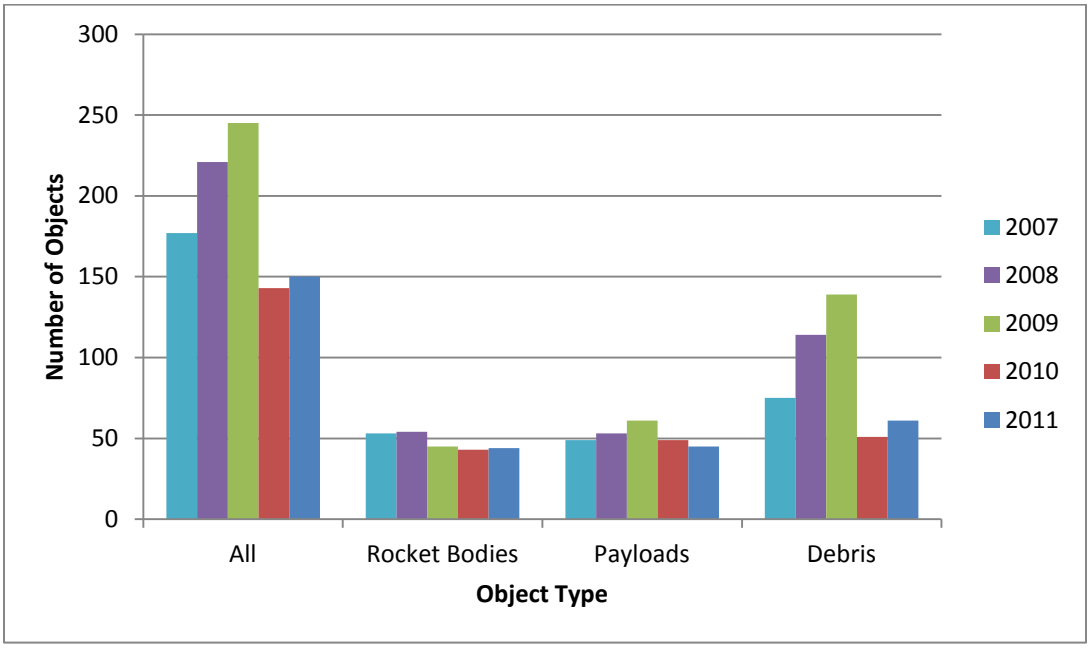

Figure 36: Objects Launched from 2007 to 2011 by Object Type

Based upon the previous last 5 years, the approximate average number of objects launched into Low-LEO by object type is as follows: 48 (26%) rocket bodies, 51 (27%) payloads, and 88 (47%) debris. Therefore, the average number of non-active RSOs (debris and rocket bodies) launched into Low-LEO each year is approximately 136 objects (48 rocket bodies plus 88 debris). For the purposes of this analysis, 136 RSO was assumed to be the maximum number of RSOs launched into Low-LEO that could potentially include a PACS payload.

In order to estimate the average length of time on orbit for objects launched into Low-LEO, the time on orbit for rocket bodies launched into Low-LEO during the 1990s were studied. In the 1990s (time period of 1 Jan 1990 to 31 Dec 1999) there were a total of 833 rocket bodies launched into Low-LEO. A certain percentage of these 833 objects returned to Earth within a month (~29%), where a certain percentage (~30%) were still

on orbit (as of 15 November 2012). A graph of the time on-orbit for these rocket bodies is seen is Figure 37.

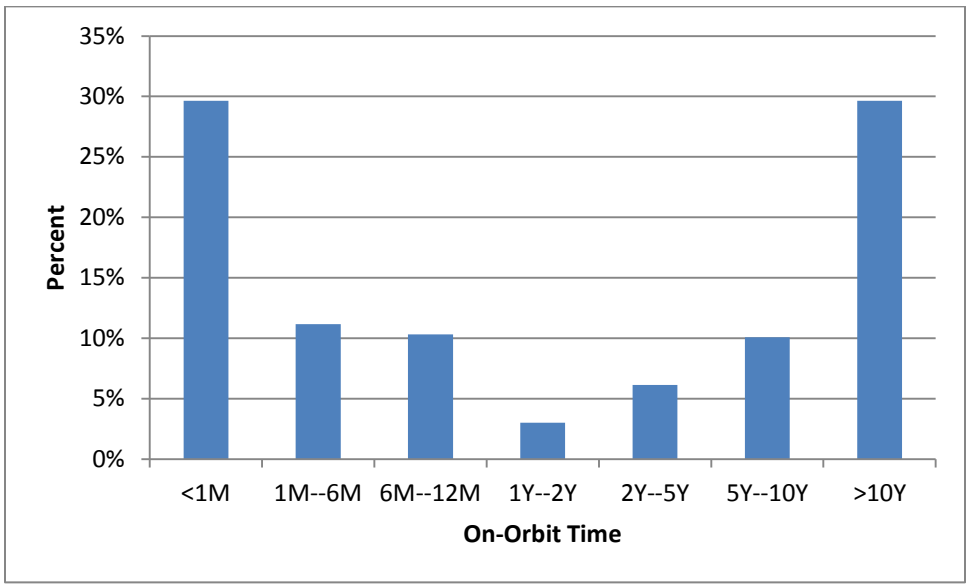

Figure 37: Time On Orbit for Rocket Bodies Launched from 1 Jan 1990 to 31 Dec 1999. 833 Total Objects. Represented in Months (M) and Years (Y).

By using the data represented in Figure 37, an estimation of time on orbit for future RSOs launched into Low-LEO was made. Table 13 shows the estimated time in orbit for these specific RSOs by percentage. This estimation was based upon data obtained from Figure 37. For example, it was assumed that 29% of RSOs launched into Low-LEO were on orbit for exactly 1 month. This 29% corresponds to 40 objects out of the estimated 136 RSOs (debris and rocket bodies) launched into Low-LEO each year.

Table 13: Estimated Time on Orbit for RSOs

Estimated Time on Orbit (Months)	% of RSO	Number of RSOs (out of 136)
1	29	40
3	11	15
9	10	14
18	3	4
42	6	8
90	10	14
Over 120	30	41

In summary, for this model it is assumed that there are 136 RSOs (debris or rocket bodies) launched into Low-LEO per year (and for simplicity, all launches occur on 1 January of each year). Additionally, the time on orbit for these objects are set based upon the numbers in Table 12. Using the spreadsheet and graphing capabilities of EXCEL, the total number of RSO that could include a PACS payload is graphed in Figure 38.

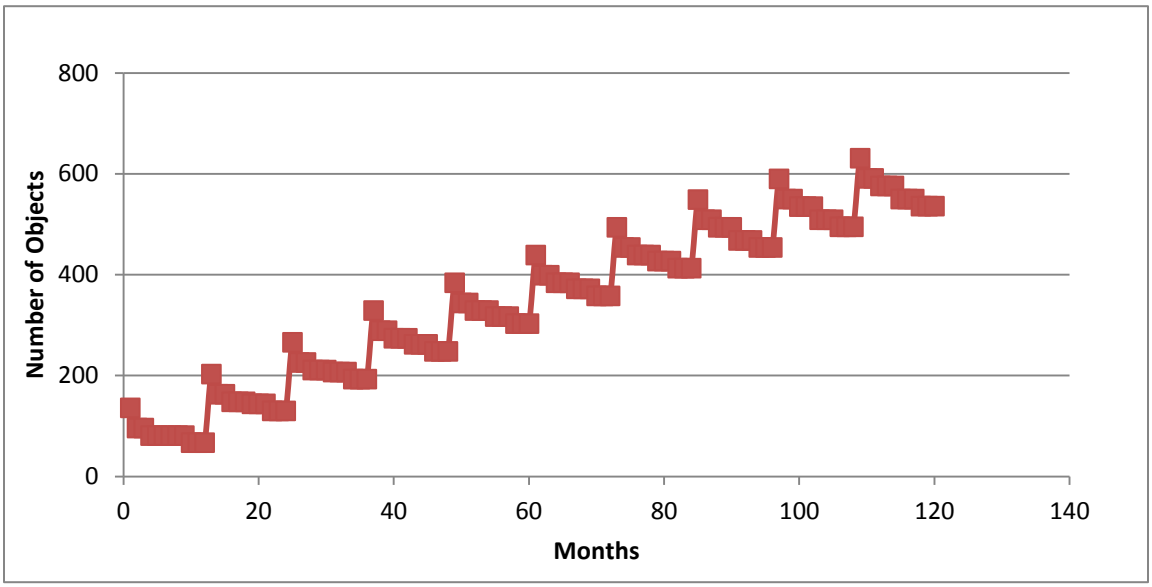

Figure 38: Potential Number of Objects with PACS assuming a 100% Placement Level over a 10 Year Period

At the end of 10 years it is estimated that if every piece of debris or rocket body that launched into Low-LEO had a PACS payload attached (100% Placement Rate), then there could potentially be approximately 536 PACS enabled objects in Low-LEO. This would require approximately 1360 PACS payloads being attached to RSOs (136 per year for 10 years).

Obviously, a 100% placement rate of PACS payloads on RSOs being launched may not be possible. For instance, the majority of RSOs launched into Low-LEO are not launched by the United States. Some countries may be more interested than others to include PACS payloads on their RSO. Also, due to physical constraints not all objects may be capable of incorporating a PACS payload. For example, if the RSO extremely small or oddly shaped.

Figure 39 below is a chart representing the objects launched in 2011 into Low-LEO. There were 150 total objects launched in 2011 and 18 of them were launched by the United States (approximately 12%). The countries that launched the most RSOs were China with 54 objects and the Commonwealth of Independent States (CIS – which includes the country of Russia) with 56 RSOs. Therefore, in 2011 approximately 73% of the objects launched into Low-LEO were launched by either the Chinese or the Russians (or more precisely the CIS).

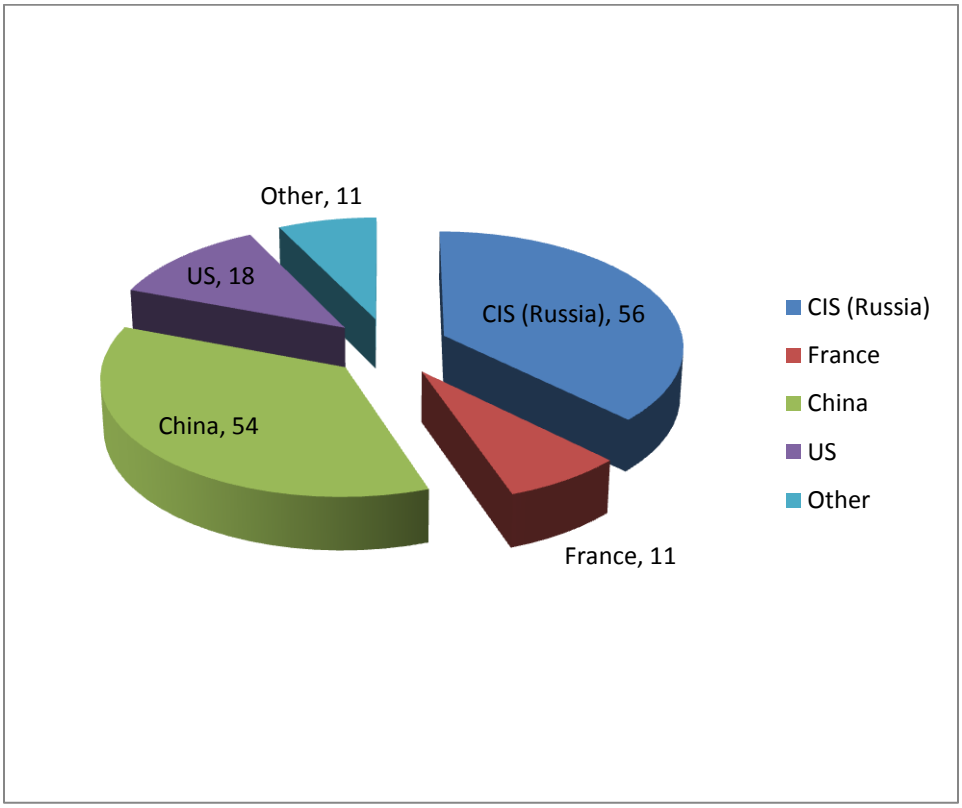

Figure 39: All Objects Launched into Low-LEO by Country in 2011

Additionally, Figure 40 below shows the number of objects launched by country for the years 2007 to 2011. Over this 5 year period, the US launched approximately 13% of the RSOs into Low-LEO.

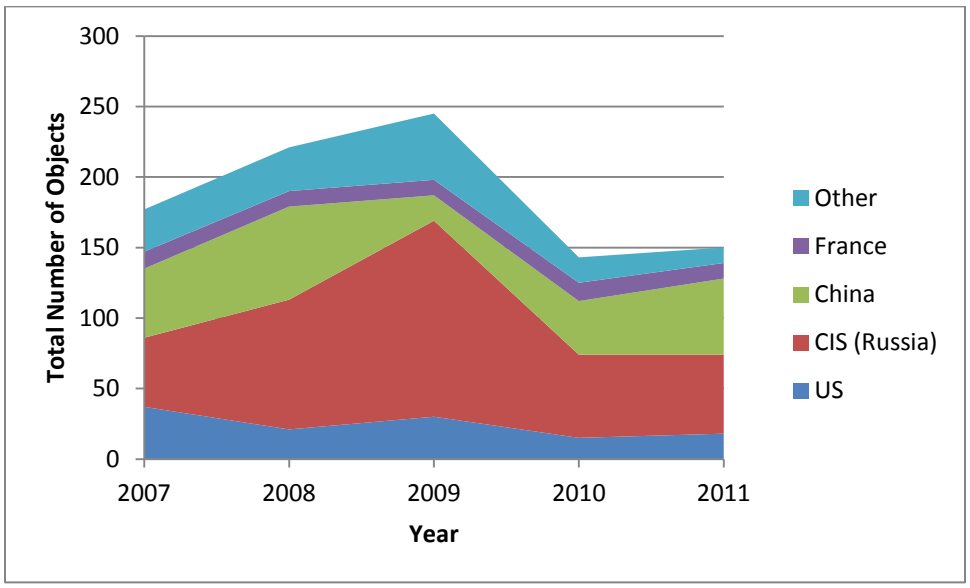

Figure 40: Total Objects Launched into Low-LEO by Country

The estimation of 536 PACS-enabled objects at the end of a 10 year period is based upon a 100% placement level. However, since a 100% placement level may not be possible, varying placement levels were assumed: 100%, 50%, 13% (based upon the percentage of RSOs launched by the United States), and 1%. The results can be seen in Figure 41. The total number of RSOs in Low-LEO was calculated to be 6119 objects (based upon data downloaded from the www.beta.space-track.org website on 15 November 2012) and for purposes of this model was held constant throughout the 10 year period. As already discussed, assuming a 100% placement rate, 536 PACS-enabled objects could be in orbit at the end of the 10 years. Assuming that the total number of

non-active objects in Low-LEO is constant over the 10 year period at 6119, these 536 RSO would represents approximately 8.7% of the total debris in Low-LEO. If the placement rate was 50%, then there would be approximately 268 PACS-enabled RSOs in Low-LEO (~4.3%). A 13% placement rate would represent approximately 70 PACS-enabled RSOs (~1.1%). A 1% placement rate would represent approximately 5 PACS-enabled RSOs (~0.1%).

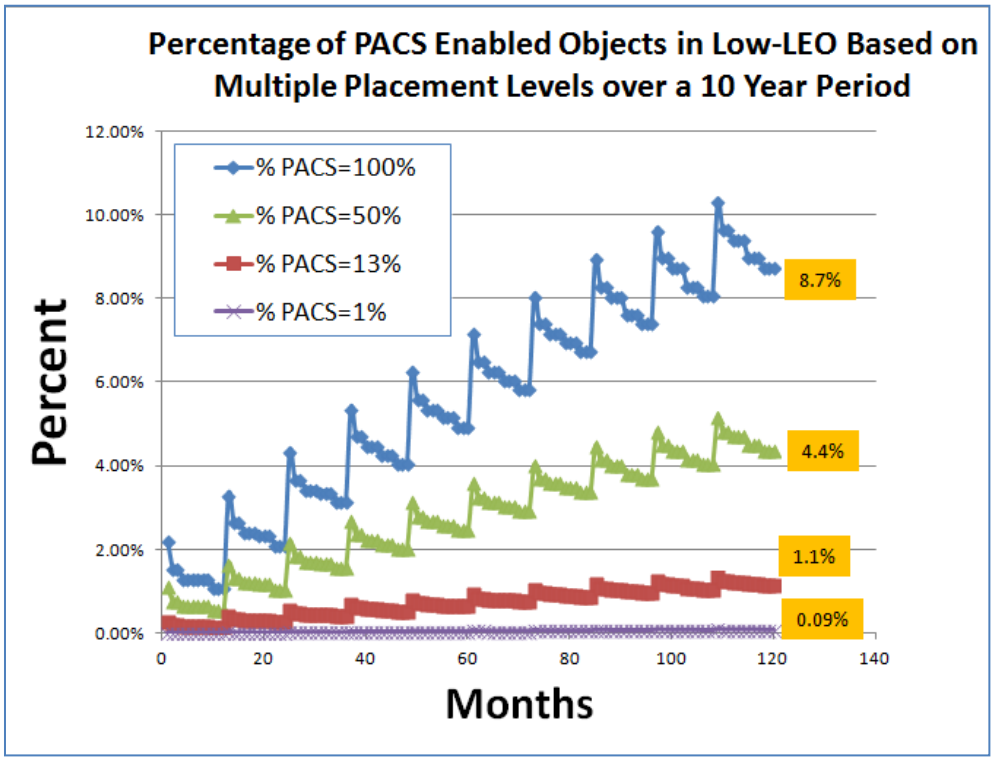

Figure 41: Percentage of PACS-Enabled Objects in Low-LEO Based upon Multiple Placement Levels Over a 10 Year Period

4.9 Frequency of Conjunctions in Low-LEO

In evaluating the impact of the PACS system to the conjunction analysis performed by JSpOC, it is important to understand the frequency in which PACS enabled RSO may experience a near conjunction. For example, the potential benefits of the PACS system will be very different if the associated RSO only experiences an identified conjunction once a year versus once a month versus many times a day. Therefore some analysis was performed to quantify how often (on average) a RSO in Low-LEO experiences an identified conjunction.

To quantify and understand the number of conjunctions per year a RSO experiences, the researchers asked JSpOC the number of CSM that they identified during the 2011 calendar year. The specific questions asked and the responses are seen in Table 14.

Table 14: Questions and Answers from JSpOC Relating to Conjunctions in 2011

1	What was the number of CSMs in 2011 involving satellites in Low-LEO (below 750 km perigee)?	1137
2	Approximate number of unclassified active satellites tracked by JSpOC in 2011 in Low-LEO?	260
3	Number of JSpOC known collision avoiding maneuvers in 2011?	11

JSpOC responded that they produced 1137 CSMs in 2011 that involved RSOs in Low-LEO. They also reported that there were approximately 260 active satellites tracked in 2011 in Low-LEO. For this model assumed that the only type of collision that can occur is active RSO on non-active RSO since the ratio of inactive RSO to active RSO is very high at approximately 25:1 (6119/260). Making this assumption, on average each active satellite experienced approximately 4.37 conjunctions per active satellite per year

(1137 divided by 260). Obviously, some RSOs likely had many more conjunctions and others had fewer. Additionally, the approximate frequency that a non-active satellite (i.e. rocket body or piece of debris) has a CSM was calculated. Since there were approximately 1137 CSMs in Low-LEO in 2011, and there are approximately 6119 non-active RSOs in Low-LEO (a total number of RSOs calculated from www.beta.space-track.org (6379) in Low-LEO minus the number of active satellites (260) received from JSpOC), on average there was approximately 0.19 CSMs per RSO per year (1137 divided by 6119). Accordingly, an active satellite experiences a CSM approximately once every 0.23 years (260 divided by 1137). A piece of debris experiences a CSM approximately every 5.38 years (6119 divided by 1137). Therefore, active satellites have an identifiable CSM much more often (on average) than pieces of debris.

Not all CSMs represent a conjunction of equal risk. For example the POCs for the 10 historic conjunctions range from 2.27E-4 to 0. If it is assumed that a conjunction is considered a "serious threat" when the POC is greater than 1E-5 (1 in 10,000), then there were a total of two conjunctions (2 out of the 10) that were a conjunction of a serious threat (CST). Therefore, for the purposes of this study it is assumed that 20% of CSMs are CST. This represents 20% of the 1137 CSMs, or approximately 227 CSTs per year. If there were 227 CST per year, then an active satellite has approximately 0.87 CSTs per year (260/227) or approximately one per year. Debris would expect to experience 0.04 CSTs per year (227/6119) or once every 27 years.

Thus far the research has shown that active RSOs experience CSMs much more often than in-active RSOs. However, the research has also shown that the PACS system

makes more of a difference to a specific conjunction when the PACS payload is on the active RSO (asset) instead of the inactive RSO (debris). As previously demonstrated in this chapter, it is assumed that the PACS payload will make a difference to the conjunction 90% of the time when the payload is on the inactive RSO and 10% of the time if it is on the active RSO (assuming the conservative estimate of PACS-L). Therefore, it is estimated that a PACS payload will make a significant difference on an active RSO approximately 0.08 CSTs per year (227*0.1/260) or once every 11.4 years. It is also estimated that a PACS payload will make a significant difference on an inactive RSO (debris) approximately 0.02 CST per year (227*0.9/6119) or once every 30.7 years.

Finally, to quantify the overall impact of the PACS system, the number of future conjunctions that could be assisted by a PACS payload was calculated using several assumptions. Three primary assumptions were made: 1) 8.7% of debris in Low-LEO has a PACS payload 2) all conjunctions involve an active satellite on debris 3) PACS is beneficial to conjunction analysis 90% of the time when on the debris. By making these assumptions, it was estimated that if there were 227 CST per year, then PACS would significantly impact approximately 18 of those conjunctions (18 = 227*0.9*8.7) - reducing the number of CST from 227 to 209. If instead, the PACS payloads were on 8.7% on the assets in Low-LEO (10% effective), then PACS would impact approximately 2 conjunctions per year (227*0.1*8.7) – reducing the number of CSTs from 227 to 225.

V. Conclusions

5 Chapter Overview

This chapter describes the conclusions for this thesis based upon the results presented in the previous chapter. Also included are the recommendations for future work to study the PACS system.

5.1 Summary

This thesis covered a novel method to self report orbital information to JSpOC for certain RSOs. Decreasing the orbital uncertainty of orbiting space objects is becoming more important as the number of orbiting objects continues to increase and the likelihood of space collisions continues to rise. This PACS system will augment the existing JSpOC capabilities to track RSOs and will therefore assist in the conjunction analysis performed by JSpOC. To understand the impact that the PACS system could potentially have on the conjunction analysis that is currently performed by JSpOC, a model was created that demonstrated that the addition of a PACS payload made a large impact to the conjunction analysis if originally the uncertainty of the involved RSO is large. The systems architecture operational views developed as part of this thesis lays the groundwork for future architectural views to be created which will ensure that the PACS system is developed in the correct fashion.

5.2 DoDAF Architecture for PACS

As part of this thesis several Operational Views (OV) were created that show how the developed system may be potentially operated in the future. These architectural views can be seen in Chapter 3. The OV-1 demonstrates the high-level graphic of all of

the primary systems needed to operate the PACS system. The OV-2 shows how the data will flow through the primary systems. The OV-5a gives a hierarchal structure of all of primary activities that need to be performed by the system. In the hierarchal structure of the OV-5a, the highest level activity of the PACS system is to "Provide RSO Orbital Information to JSpOC." Finally, the OV-6c architecture views trace the necessary actions of two operational scenarios (Periodic and On-Demand).

5.3 Accuracy of Conjunction Analysis

As seen in the results section of this thesis (Chapter 4), the probability of collision calculation for most conjunctions dramatically changes with the inclusion of a PACS payload on the secondary object (debris). For the 10 conjunctions studied, it is seen that the largest impact to the POC occurs when the RSO that is including the PACS payload is poorly tracked. For example, the POC will be improved dramatically if the initial uncertainty is very large (i.e. hundreds of meters) and the inclusion of the PACS payload reduces the uncertainty to only a few, or dozens, of meters (as represented as PACS-S or PACS-L). In this case, the uncertainty is reduced dramatically. However, if the uncertainty is already very low (a few or dozens of meters) then the change to the uncertainty will not be as significant and therefore the change to the POC will not be as significant.

In the 10 conjunctions studied, the primary object (the active satellite) is tracked better by the JSpOC than the secondary objects (non-active RSOs) in 8 out of the 10 cases (where the 1-sigma in-track uncertainty at the time of conjunction of the secondary object is greater than that of the primary object). Additionally, the primary object is

tracked significantly better in 5 out of 10 of the cases (where the 1-sigma in-track uncertainty at the time of conjunction of the secondary object is ten times greater than that of the primary object).

The implementation of a PACS payload to a RSO will have the largest impact to the conjunction analysis when the "As-Is" (without a PACS payload) covariance matrix is large. If the uncertainty (covariance matrix) is already relatively small, then the shrinking of that covariance matrix by hosting a PACS payload will not decrease the summed covariance matrix (summation of the covariance matrices of the primary and secondary RSOs) nearly as much as if the RSO has a large original covariance matrix.

Therefore, since on average the covariance matrices of debris is much larger than that of active satellites, the largest impact to the conjunction analysis will typically be when the PACS payload is on the debris (as opposed to being on the asset). However, as will be discussed in the next section, a piece of debris will experience (on average) far fewer conjunctions (as defined as a JSpOC reported CSM) per year than an active satellite.

5.4 Projected Future Number of RSOs in Low-LEO

One key question of this thesis was to approximate the number of RSOs that could potentially have a PACS payload on it after a certain period of time. For this analysis a ten year time period (ten years after the system goes operational) was chosen. Based upon the methodology and results in the previous chapters, it is estimated that if a PACS payload was put on every non-active RSO being launch into Low-LEO then a total

of approximately 536 objects could have a PACS payload on it after a ten year period. This represents approximately 8.7% of the objects in Low-LEO.

Because a 100% placement rate of PACS payload may not be achievable (due to the reluctance of the launching country or the size/shape of the RSO), the number of RSOs with PACS was estimate at different placement levels. For example, a 13% placement rate would represent approximately 70 PACS-enabled RSOs (~1.1%). A 1% placement rate would represent approximately 5 PACS-enabled RSOs (~0.1%).

5.5 Frequency of Collisions for PACS Enabled RSOs

One of the primary goals of the research for this thesis was to estimate how often PACS enabled objects experience a close conjunction (as defined as CSM). At the beginning of this research, it was unknown to the researchers whether the conjunction frequency would be anywhere from hundreds of times per day to only a few per decade. Fortunately, JSpOC keeps records on the number of unclassified CSMs reported per year. In 2011 for example, there were 1137 CSMs in Low-LEO. As described in Chapter 4, this translates to approximately 4.37 CSMs per active satellite per year (1137 CSMs divided by 260 active satellites) and approximately 0.19 CSMs per non-active space debris per year (1137 CSMs divided by 6119 non-active RSOs). Therefore, active satellites experience a reportable conjunction much more often (on average) than an inactive RSO.

5.6 Future Work

As the PACS system matures in its development, a full DoDAF architecture framework will need to be created. This framework will expand upon the several operational views created as part of this research.

One of the primary limitations in this research is that the exact capabilities of the future PACS system to determine the orbital position of a RSO were largely unknown. This limitation is due to several reasons, including: 1) the system had not been tested operationally and therefore there was no operational data to reference; 2) the exact operational usage of the system has not yet been defined; 3) the propagation uncertainty growth rate of an RSO was not determined. As discussed earlier in this paper, due to these limitations, the PACS payload capabilities were modeled using PACS-S and PACS-L. For future research work, the capabilities of the PACS system will need to be better defined. In part, this may be accomplished by studying the propagation growth of uncertainty of RSOs in Low-LEO. One possible way to better define this propagation growth would be to work directly with the JSpOC to better understand the way in which JSpOC propagates the error growth for RSOs. As an alternative, the software package Systems Tool Kit (STK) may provide the capabilities to propagate the covariance matrices for certain RSOs. By better understanding the error propagation growth rate of RSOs in Low-LEO, the impact of the PACS system to the conjunction analysis performed by JSpOC will be improved.

Appendix 1: MATHCAD Code to Calculate the Probability of Collision

Step 1: Find the OrthoNormal Coordinate System for the UVW in the TDR (EFG) Frame for both objects and create the Rotation Matrix

Asset:

$$InertialVA := AvvTDR + ER \cdot \begin{pmatrix} 0 \\ 0 \\ 1 \end{pmatrix} \times ApvTDR$$

Equation 5 in Thesis Body

$$uA := \frac{ApvTDR}{|ApvTDR|}$$

Equation 6 in Thesis Body

$$wA := \frac{ApvTDR \times InertialVA}{|ApvTDR \times InertialVA|}$$

Equation 6 in Thesis Body

$$vA := \frac{wA \times uA}{|wA \times uA|}$$

Equation 6 in Thesis Body

$$RMA := \begin{pmatrix} uA_0 & vA_0 & wA_0 \\ uA_1 & vA_1 & wA_1 \\ uA_2 & vA_2 & wA_2 \end{pmatrix}$$

Equation 7 in Thesis Body

Debris:

$$InertialVD := DvvTDR + ER \cdot \begin{pmatrix} 0 \\ 0 \\ 1 \end{pmatrix} \times DpvTDR$$

Equation 5 in Thesis Body

$$uD := \frac{DpvTDR}{|DpvTDR|}$$

Equation 6 in Thesis Body

$$wD := \frac{DpvTDR \times InertialVD}{|DpvTDR \times InertialVD|}$$

Equation 6 in Thesis Body

$$vD := \frac{wD \times uD}{|wD \times uD|}$$

Equation 6 in Thesis Body

$$RMD := \begin{pmatrix} uD_0 & vD_0 & wD_0 \\ uD_1 & vD_1 & wD_1 \\ uD_2 & vD_2 & wD_2 \end{pmatrix}$$

Equation 7 in Thesis Body

Step 2: Use the Rotation Matix to put the Covariance Matrices into the TDR Frame

Asset:

$$A\_CM\_TDR := RMA \cdot AcmUVW \cdot RMA^T$$

Equation 8 in Thesis Body

Debris:

$$D\_CM\_TDR := RMD \cdot DcmUVW \cdot RMD^T$$

Equation 8 in Thesis Body

Step 3: Sum the Covariance Matrices

$$S\_CM\_TDR := A\_CM\_TDR + D\_CM\_TDR$$

Equation 9 in Thesis Body

Step 4: Find the Relative Velocity Vector and Normalize it

$$RvvTDR := \frac{AvvTDR - DvvTDR}{|AvvTDR - DvvTDR|}$$

Equation 10 in Thesis Body

Step 5: Using the Gram Schmidt Method: Find the OrthoNormal Basis for the Relative Velocity Vector

$$aUnit := \begin{pmatrix} 1 \\ 0 \\ 0 \end{pmatrix} \qquad a := \frac{aUnit - (aUnit \cdot RvvTDR) \cdot RvvTDR}{|aUnit - (aUnit \cdot RvvTDR) \cdot RvvTDR|}$$

$$bUnit := \begin{pmatrix} 0 \\ 1 \\ 0 \end{pmatrix} \qquad b := \frac{bUnit - (bUnit \cdot RvvTDR) \cdot RvvTDR - (bUnit \cdot a) \cdot a}{|bUnit - (bUnit \cdot RvvTDR) \cdot RvvTDR - (bUnit \cdot a) \cdot a|}$$

Step 6: Create the Rotation Matrix to go from the TDR Frame to the Relative Velocity Frame

$$RMTDRtoVAB := \begin{pmatrix} RvvTDR_0 & a_0 & b_0 \\ RvvTDR_1 & a_1 & b_1 \\ RvvTDR_2 & a_2 & b_2 \end{pmatrix}^T$$

Equation 11 in Thesis Body

Step 7: Using the Rotation Matrix, convert the Summed Covariance Matrix into the Relative Velocity Reference Frame

$$CMVAB := RMTDRtoVAB \cdot S\_CM\_TDR \cdot RMTDRtoVAB^T$$

Equation 12 in Thesis Body

Step 8: Using the Rotation Matrix, put the Postion Difference (TDR) in the coordinate system (V, a, b)

$$RpvTDR := ApvTDR - DpvTDR$$

Equation 14 in Thesis Body

$$RpvVAB := RMTDRtoVAB \cdot RpvTDR$$

Equation 15 in Thesis Body

Step 9: Put the Covariance Matrix and Relative Position Difference into a 2-Dimension X,Y by eliminating the first row and collumn

$$CMAB := \begin{pmatrix} CMVAB_{1,1} & CMVAB_{1,2} \\ CMVAB_{2,1} & CMVAB_{2,2} \end{pmatrix}$$

Equation 16 in Thesis Body

$$RpvAB := \begin{pmatrix} RpvVAB_1 \\ RpvVAB_2 \end{pmatrix}$$

Equation 17 in Thesis Body

Step 10: Integrate over the exclusion volume.

$$POC := \frac{1}{2\cdot\pi\cdot\left(|CMAB|\right)^{\frac{1}{2}}}\cdot\int_{-EV}^{EV}\int_{-\left[EV^2-(Av)^2\right]^{\frac{1}{2}}}^{\left[EV^2-(Av)^2\right]^{\frac{1}{2}}} e^{\left[\frac{-1}{2}\cdot\left[\left[RpvAB+\begin{pmatrix}Av\\Bv\end{pmatrix}\right]^T\cdot CMAB^{-1}\cdot\left[RpvAB+\begin{pmatrix}Av\\Bv\end{pmatrix}\right]\right]\right]} dBv\, dAv$$

Equation 18 in Thesis Body

Equation 19 in Thesis Body

$$POC3 := \frac{1}{2\cdot\pi\cdot\left(|CMAB|\right)^{\frac{1}{2}}}\cdot\int_{-EV}^{EV}\int_{-EV}^{EV} e^{\left[\frac{-1}{2}\cdot\left[\left[RpvAB+\begin{pmatrix}Av\\Bv\end{pmatrix}\right]^T\cdot CMAB^{-1}\cdot\left[RpvAB+\begin{pmatrix}Av\\Bv\end{pmatrix}\right]\right]\right]} dBv\, dAv$$

Bibliography

[1] National Research Council of the National Academies, "Continuing Kepler's Quest - Assessing Air Force Space Command's Astrodynamics Standards," National Academies Press, Washington DC, 2012.

[2] J. L. William, "Remarks on Space Policy at U.S. Strategic Command Space Symposium," in *U.S. Depart*, Omaha, 2010.

[3] Department of Defense and the Office of the Director of National Intelligence, "National Security Space Strategy," DoD & DNI, Washington DC, 2011.

[4] M. W. Maier and E. Rechtin, The Art of Systems Architecting, 3rd Edition, Boca Raton: CRC Press, 2009.

[5] U.S. Department of Defense, "DoD Architecture Framework 2.02," Department of Defense, 1 August 2010. [Online]. Available: http://dodcio.defense.gov/dodaf20.aspx. [Accessed 10 November 2012].

[6] Jet Propulsion Laboratory, "GRACE: Millimeters and Microns in Orbit," Unknown, California Institute of Technology, 2002.

[7] "USSTRATCOM Space Control and Space Surveillance," United States Department of Defense, [Online]. Available: http://www.stratcom.mil/factsheets/USSTRATCOM_Space_Control_and_Space_Surveillance/. [Accessed 16 October 2012].

[8] United States Strategic Command, "USSTRATCOM Space Control and Space Surveillance," US STRATCOM, 1 May 2012. [Online]. Available: http://www.stratcom.mil/factsheets/USSTRATCOM_Space_Control_and_Space_Surveillance/. [Accessed 4 February 2013].

[9] C. M. Wasson, "Space Situational Awareness in the Joint Space Operations Center," in *Advanced Maui Optical and Space Surveillance Technologies Conference*, Kihei, 2011.

[10 JSPOC, "Conjunction Summary Message Guide," Vandenberg AFB, 2012.

[11 S. R. Pratt, C. E. Fossa and M. A. Temple, "An Operational and Performance Overview of the Iridium Low Earth Orbit Satellite System," *IEEE Communications Survey,* vol. 2nd Quarter, pp. 1-10, 1999.

[12 W. E. Wiesel, Modern Orbit Determination, Beavercreek: Aphelion Press, 2010.

[13 U. S. S. Command, "Space-Track," United States Strategic Command, [Online]. Available: https://beta.space-track.org/auth/login. [Accessed 15 November 2012].

[14 J. Wertz, D. Everett and J. Puschell, Space Mission Engineering: The New SMAD, Hawthorne: Microcosm Press, 2011.

[15 W. Cheney and D. Kincaid, Linear Algebra: Theory and Application, Sudbury: Jones and Barlett Learning, 2009.

[16 Novatel Coorporation, "Novatel Fact Sheet of the OEMV-1G," Novatel Coorporation, [Online]. Available: http://www.novatel.com/products/gnss-receivers/oem-receiver-boards/oemv-receivers/oemv-1g/. [Accessed 15 November 2012].

[17 NASA, "NASA and DARPA Sponsor International Debris Removal Conference," *Orbital Debris Quarterly,* vol. 14, no. 1, p. 1, 2010.

[18 "NASA Orbital Debris Program Office," NASA, 02 October 2012. [Online]. Available: http://orbitaldebris.jsc.nasa.gov/photogallery/beehives.html.

[19 National Research Council of the National Academies, Continuing Kepler's Quest-Assessign Air Force Space Command's Astrodynamics Standars, Washington

DC: The National Academies Press, 2012.

[20 D. A. Vallado and W. D. McClain, Fundamentals of Astrodynics and Applications, El Segundo: Microcosm Press and Kluwer Academic Publishers, 2004.

[21 J. R. Wertz, D. F. Everett and J. J. Puschell, Space Mission Engineering: The New SMAD, Hawthorne: Microcosm Press, 2011.

REPORT DOCUMENTATION PAGE		*Form Approved* *OMB No. 0704–0188*
The public reporting burden for this collection of information is estimated to average 1 hour per response, including the time for reviewing instructions, searching existing data sources, gathering and maintaining the data needed, and completing and reviewing the collection of information. Send comments regarding this burden estimate or any other aspect of this collection of information, including suggestions for reducing this burden to Department of Defense, Washington Headquarters Services, Directorate for Information Operations and Reports (0704–0188), 1215 Jefferson Davis Highway, Suite 1204, Arlington, VA 22202–4302. Respondents should be aware that notwithstanding any other provision of law, no person shall be subject to any penalty for failing to comply with a collection of information if it does not display a currently valid OMB control number. PLEASE DO NOT RETURN YOUR FORM TO THE ABOVE ADDRESS.		
1. REPORT DATE (DD–MM–YYYY) 21-03-2013	2. REPORT TYPE Master's Thesis	3. DATES COVERED *(From — To)* Mar 2012 – Mar 2013
4. TITLE AND SUBTITLE Modeling the impact of the Payload Alert Communications System (PACS) on the accuracy of conjunction analysis		5a. CONTRACT NUMBER 5b. GRANT NUMBER 5c. PROGRAM ELEMENT NUMBER
6. AUTHOR(S) Bastow, Landon B., Captain, USAF		5d. PROJECT NUMBER 5e. TASK NUMBER 5f. WORK UNIT NUMBER
7. PERFORMING ORGANIZATION NAME(S) AND ADDRESS(ES) Air Force Institute of Technology Graduate School of Engineering and Management (AFIT/ENY) 2950 Hobson Way WPAFB OH 45433-7765		8. PERFORMING ORGANIZATION REPORT NUMBER AFIT-ENV-13-M-01
9. SPONSORING / MONITORING AGENCY NAME(S) AND ADDRESS(ES) Mr Stephen Lucero Air Force Research Lab Space Vehicles Directorate 3550 Aberdeen Ave SE Bldg 592 Rm 103 Kirtland AFB, NM 87117-5776 stephen.lucerco@kirtland.af.mil 505-846-4137		10. SPONSOR/MONITOR'S ACRONYM(S) AFRL/RV 11. SPONSOR/MONITOR'S REPORT NUMBER(S)
12. DISTRIBUTION / AVAILABILITY STATEMENT DISTRIBUTION STATEMENT A: APPROVED FOR PUBLIC RELEASE; DISTRIBUTION IS UNLIMITED		
13. SUPPLEMENTARY NOTES This material is declared a work of the U.S. Government and is not subject to copyright protection in the United States.		
14. ABSTRACT The Air Force Institute of Technology (AFIT) and the Air Force Research Laboratory (AFRL) are jointly developing a system known as the Payload Alert Communications System (PACS) whose purpose is to decrease the statistical uncertainty in the location of resident space objects (RSOs). PACS is designed to augment the Joint Space Operations Center's (JSpOC) existing space object tracking capabilities which is expected to increase the accuracy of conjunction estimation. In the current PACS design, a small payload would be attached to certain RSOs prior their launch. It is envisioned that this payload would basically consist of a microcontroller, a Global Positioning System (GPS) receiver, a communication transceiver, and a power source. Once on orbit, the PACS payload would collect GPS position information and then periodically, or upon demand, transmit the orbital information back to JSpOC. In this thesis, a study is performed to determine how the accuracy of conjunction analysis performed by the JSpOC would be impacted when RSOs are equipped with PACS. This effort requires the development an initial PACS system architecture, formulation of the mathematical models used in conjunction analysis, and the simulation and analysis of conjunction analysis under various scenarios.		
15. SUBJECT TERMS Conjunction Analysis; Space; Collisions; Covariance Matrix		

16. SECURITY CLASSIFICATION OF:			17. LIMITATION OF ABSTRACT	18. NUMBER OF PAGES	19a. NAME OF RESPONSIBLE PERSON Dr. Michael Grimaila
a. REPORT U	b. ABSTRACT U	c. THIS PAGE U	UU	119	19b. TELEPHONE NUMBER (Include Area Code) (937)255-3636, ext 4800 (michael.grimaila@afit.edu)